RSC Sustainability

Accepted Manuscript

This article can be cited before page numbers have been issued, to do this please use: P. Wang, Y. Qin, L. Wang, T. Qi and F. Meng, *RSC Sustainability*, 2025, DOI: 10.1039/D5SU00532A.

View Article Online
DOI: 10.1039/D5SU00532A

Sustainability Spotlight Statement

Vanadium flow batteries (VFBs) are vital for integrating renewable energy and enabling grid decarbonization. However, the economic and environmental costs of preparing their essential $V^{3.5+}$ electrolyte pose significant barriers to sustainable VFB deployment. This review critically analyzes $V^{3.5+}$ electrolyte synthesis methods, highlighting pathways to reduce resource consumption, minimize waste, and lower production energy intensity. By advancing efficient, low-impact electrolyte manufacturing and capacity restoration techniques, this work directly contributes to making large-scale, long-duration energy storage more affordable and environmentally sound. These advancements align with key UN Sustainable Development Goals: **SDG 7 (Affordable and Clean Energy)** by enabling renewable storage, **SDG 9 (Industry, Innovation and Infrastructure)** through cleaner production innovation, and **SDG 12 (Responsible Consumption and Production)** by promoting resource efficiency and waste reduction in battery value chains.

View Article Online
DOI: 10.1039/D5SU00532A

Preparation methods of $V^{3.5+}$ electrolyte and related capacity recovery strategies for vanadium flow batteries: A review

Pai Wang[a,b], Yu Qin*[,c], Lina Wang[a,b], Tao Qi[a], Fancheng Meng*[,a,b]

[a] *National Engineering Research Center of Green Recycling for Strategic Metal Resources, Institute of Process Engineering, Chinese Academy of Sciences, Beijing 100190, China*

[b] *School of Chemical Engineering, University of Chinese Academy of Sciences, Beijing 101408, China*

[c] *Shenyang Hengjiu Antai Environmental Protection and Energy Conservation Technology Co., Ltd, Shenyang 110127, China*

*Corresponding authors:

E-mail address: qiny@h9at.com (Y. Qin); Full postal address: No.158, Puhe Road, Shenbei New District, Shenyang, Liaoning Province, China; Telephone number: +86-024-85635968.

E-mail address: fcmeng@ipe.ac.cn (F. Meng); Full postal address: No.1, North 2nd Street, Zhongguancun, Haidian District, Beijing, China; Telephone number: +86-010-82544848

View Article Online
DOI: 10.1039/D5SU00532A

Abstract

Vanadium flow battery (VFB) represents a prominent large-scale long-duration energy storage technology, with vanadium electrolyte serving as a critical component that fundamentally governs battery performance. In practical implementations, mixed-valence $V^{3.5+}$ electrolyte is universally employed as the initial active solution in both half-cells. The preparation methodology and raw material selection for $V^{3.5+}$ electrolyte substantially influence both the economic viability and environmental sustainability of VFB systems. This review systematically examines established techniques for preparing $V^{3.5+}$ electrolyte, including chemical reduction method, electrolysis method, chemical reduction-electrolysis method, and further classifies them systematically, analyzes the basic principles, process architecture, key equipment, technical advantages and existing problems of each process, and discusses the potential of each method in sustainable application. In addition, this study also analyzed the capacity attenuation mechanism of vanadium battery, and summarized the capacity recovery strategy. The reduction process of high valence vanadium ions involved in the capacity recovery process and the preparation of $V^{3.5+}$ electrolyte have high commonality in chemical principle and process technology. The review concludes with a forward-looking perspective on technological innovations in electrolyte synthesis, emphasizing sustainable production routes and performance optimization strategies for next-generation VFB applications.

Keywords: $V^{3.5+}$ electrolyte; Preparation method; Sustainable development; Capacity recovery

View Article Online
DOI: 10.1039/D5SU00532A

1 Introduction

Renewable energy sources are receiving widespread attention because of the existing fossil fuel-based energy infrastructure cannot meet the requirements of sustainable social development[1, 2]. The VFB stands out as a mature large-scale energy storage technology[3-5], which is recognized as one of the most advanced energy storage technologies today, it offers advantages such as long cycle life, flexible design, and safe system operation[6-8]. Pioneered by the University of New South Wales in the 1980s[9, 10], the VFB achieves mutual conversion between chemical energy and electrical energy through reversible changes in the valence states of vanadium ions in sulfuric acid electrolyte: during charging, electrical energy is converted into chemical energy for storage, while during discharging, chemical energy is reconverted into electrical energy for output**.** Its energy storage principle and energy conversion during the charge-discharge process are shown in Fig. 1. This unique single-element design eliminates cross-contamination through membrane infiltration theoretically[11]. When the battery is charged, the anode undergoes an oxidation reaction, and V^{4+} loses electrons and is oxidized to V^{5+}. At the same time, a reduction reaction occurs at the negative electrode, and V^{3+} gains electrons and is reduced to V^{2+}. These electrons flow through an external circuit to charge the battery. During the whole charging and discharging process, H^{+} ions in the positive and negative solutions migrate through the proton exchange membrane to maintain the charge balance[12]. The reaction equations for the discharging process are shown by Eq. (1-3)[13, 14] while the charge process is the reverse of these reactions. :

View Article Online
DOI: 10.1039/D5SU00532A

Positive: $VO_2^+ + 2H^+ + e^- = VO^{2+} + H_2O$ E_0=1.00 V (1)

Negative: $V^{2+} = V^{3+} + e^-$ E_0=−0.25 V (2)

Net: $VO_2^+ + 2H^+ + V^{2+} = VO^{2+} + V^{3+} + H_2O$ E_0=1.25 V (3)

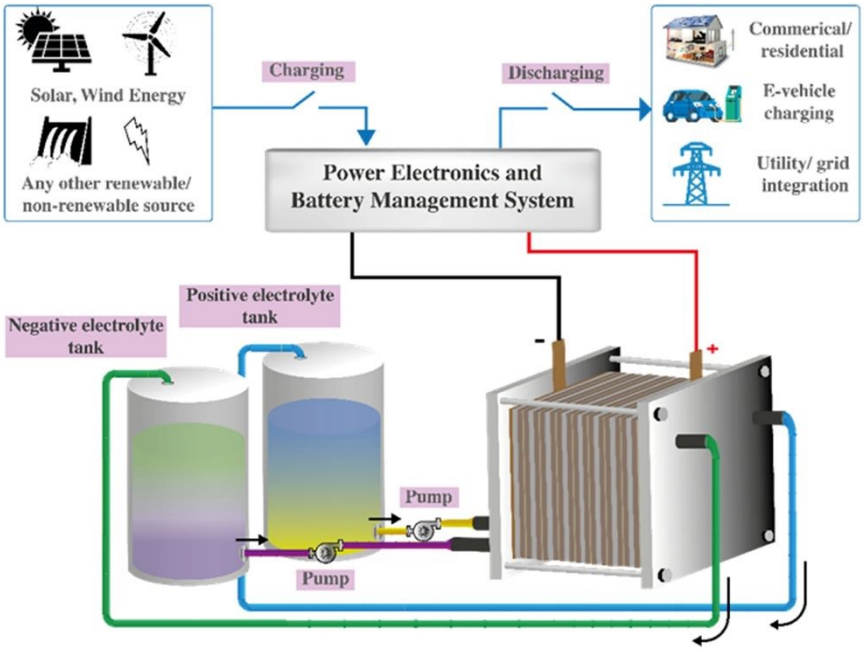

Fig. 1. VFB energy storage schematic[15](Reprinted with permission of Spinger Nature)

As the energy carrier of VFB, the vanadium electrolyte is one of the key materials and its performance and quality are the key to the safe operation of VFB over a long period of time[16].The $V^{3.5+}$ electrolyte refers to an electrolyte in which the average valence state of vanadium ions is 3.5, meaning it is an equimolar mixture of V^{4+} and V^{3+} ions as the initial valence states for the positive and negative electrolytes[17]. The $V^{3.5+}$ electrolyte, as the initial electrolyte, exhibits symmetric valence state changes, and the transfer of electrons and ions during the reaction process is mutually balanced, thus eliminating the need for additional adjustments to the positive and negative electrode capacities. The preparation of vanadium electrolyte involves the conversion of different valence vanadium ions, and vanadium electrolyte is usually prepared with high-purity

View Article Online
DOI: 10.1039/D5SU00532A

V_2O_5 (purity > 99.5%) as the raw material[18, 19] The amount of electrolyte can even reach hundreds of tons in the megawatt VFB system, and the cost of vanadium electrolyte generally accounts for more than 50% of the total cost of VFB energy storage system[12]. Generally, the cost of vanadium electrolyte is determined by the raw materials and preparation methods[20, 21]. Besides, the long-term operational challenges of VFB primarily stem from electrolyte concentration decay, volume changes and valence state imbalances[22, 23], which collectively contribute to capacity fading over time[24-27]. The adjustment of the valence state of vanadium ions, the recovery of electrolyte capacity and recycling are the key to realizing the economy and sustainability of the VFB storage system.

In this review, we systematically present the classification and critical evaluation of modern methodologies employed in the preparation of $V^{3.5+}$ electrolyte. A comprehensive review of the primary synthesis techniques such as chemical reduction method, electrolysis method, chemical reduction-electrolysis method are conducted. Special attention is given to the selection of vanadium precursors and valence state manipulation. Furthermore, this review addresses the capacity fading issues while providing a comprehensive summary of capacity restoration strategies for vanadium electrolytes.

2. Chemical properties of $V^{3.5+}$ electrolyte

2.1 $V^{3.5+}$ electrolyte composition and stability

In practical application, there are detailed requirements for the concentration of vanadium ions and sulfuric acid in $V^{3.5+}$ electrolyte, and the requirements for impurity

View Article Online
DOI: 10.1039/D5SU00532A

content are more stringent. V^{2+} ions are unstable and prone to oxidation reactions, while V^{5+} ions tend to form precipitates. In contrast, V^{3+} and V^{4+} ions are relatively stable, with stability data shown in Table 1. This is one of the main reasons why vanadium electrolyte is prepared, stored, transported and initially installed in the form of $V^{3.5+}$ electrolyte.

Table 1 Stability of V^{n+} sulfate solutions[28]

V^{n+} species	V^{n+}, M	Total sulfate, M	T, ℃	Time
V^{3+}	2.0	5.0	−5	Stable(>10d)
	2.0	5.0	25	Stable(>10d)
	2.0	5.0	40	Stable(>10d)
V^{4+} (VO^{2+})	2.0	5.0	−5	18hr
	2.0	5.0	25	95hr
	2.0	5.0	40	Stable(>10d)

$V^{3.5+}$ electrolytes typically utilize sulfuric acid as the primary supporting electrolyte, with sulfate ions acting as the coordinating ligands. The common composition of the electrolyte consists of vanadium ion concentrations ranging from 1.5 to 1.8 mol/L and sulfate ion concentrations between 4 and 5 mol/L shown in Table 2. The dual functionality of H_2SO_4 as both a proton donor and a coordinating medium enhances the stability and ionic conductivity of the electrolyte. Chloride and phosphate ions inhibit vanadium ion aggregation through competitive coordination, thereby inhibiting aggregation and enhancing colloidal stability and the reversibility of redox reactions, thus HCl and mixed acids such as H_2SO_4-HCl and H_2SO_4-H_3PO_4 are used as

View Article Online
DOI: 10.1039/D5SU00532A

the supporting electrolytes and their typical compositions of vanadium electrolyte. The introduction of HCl electrolyte can improve the solubility of vanadium ions and the thermal stability of electrolyte, but there is a great risk of chlorine leakage and equipment corrosion in actual use. Optimizing the electrolyte concentration within different acid systems can significantly improve the temperature adaptability and energy density of VFB.

Table 2 Composition of vanadium electrolytes in different systems

	V, M	Sulfate ions, M	HCl, M	H_3PO_4, M
H_2SO_4	1.5-2.0	4.0-5.0	/	--
HCl[29, 30]	1.5-2.5	/	5.0-6.0	/
H_2SO_4+HCl[31, 32]	2.5-3.0	2.0-3.0	5.5-6.5	/
H_2SO_4+H_3PO_4[33]	1.5-2.0	3.0-3.5	/	0.1-1.0

2.2 Solvation structures of vanadium ions in $V^{3.5+}$ electrolytes

Vanadium ions exhibit complex speciation in aqueous solutions, with its oxidation states and stability highly dependent on pH and electrode potential as shown in Fig. 2. Under acidic conditions, vanadium can exist in four ionic forms, including V^{2+}, V^{3+}, VO^{2+}, and VO_2^+. The dominant ions at low potentials are V^{3+} and VO^{2+}, whereas when the potential exceeds approximately 0.8V, the dominant ions shift to VO^{2+} and VO_2^+.This indicates that in strongly acidic solutions of $V^{3.5+}$ electrolyte, vanadium ions primarily exist in the forms of $VO^{2+}$and V^{3+}.

As for $V^{3.5+}$ electrolyte, the most stable configurations formed by $V^{3+}$and V^{4+} ions

View Article Online
DOI: 10.1039/D5SU00532A

in different acid solutions are presented in Fig. 3. It shows that V^{3+} ion forms hexahydrate structures with an octahedral geometry denoted as $[V(H_2O)_6]^{3+}$[34-36]. The VO^{2+} ion adopts a pentahydrate structure, forming an octahedral geometry with one vanadyl oxygen and five water molecules represented as $[VO(H_2O)_5]^{2+}$[37-42]. These structures highlight the influence of charge density and oxidation state on the coordination chemistry of vanadium ions.

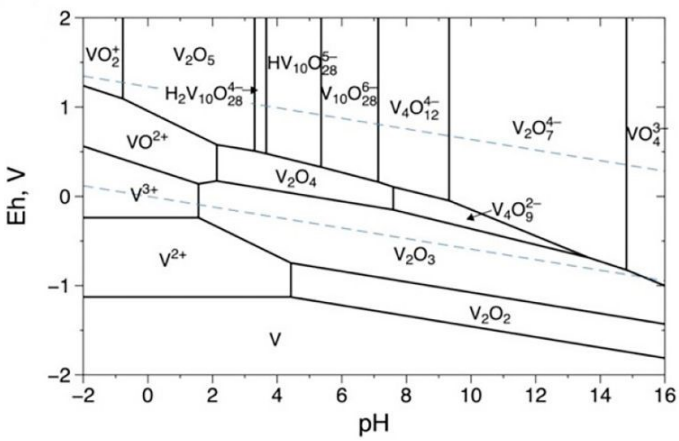

Fig. 2. Eh–pH diagram for vanadium species at [V]=1M[43](Reprinted with permission of American Chemical Society)

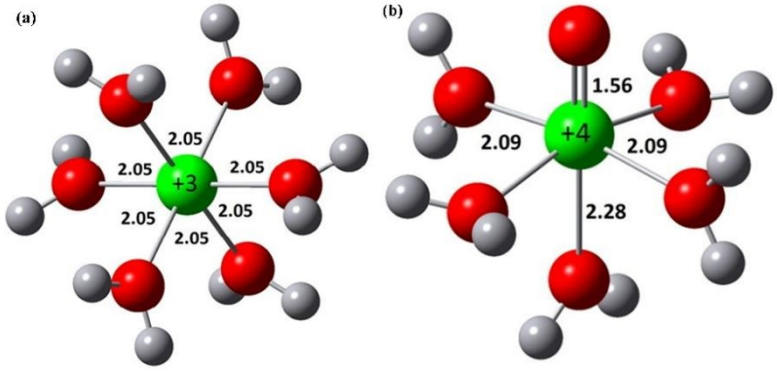

Fig. 3 Structures of (a) $V^{3+}$and (b) V^{4+} ions and their first solvation shell water molecules by DFT[44] (Reprinted with permission of Elsevier)

2.3 Basic redox reactions of preparing $V^{3.5+}$ electrolyte

The preparation of $V^{3.5+}$ electrolyte from pentavalent vanadium is essentially a

View Article Online
DOI: 10.1039/D5SU00532A

step-by-step reduction process: firstly, V^{5+} is reduced to V^{4+}, and then V^{4+} is further reduced to V^{3+}. The conventional method is to dissolve V_2O_5 in sulfuric acid aqueous solution and use oxalic acid[45-47], acetic acid[48], sulfur dioxide[49] or glycerol[50] as reducing agents to prepare $V^{3.5+}$ electrolyte[51]. However, these traditional reductants can only realize the transformation from V^{5+} to V^{4+} in the water phase environment, and cannot continue to reduce V^{4+} to V^{3+} due to their reducing ability. Therefore, the realization of efficient and deep reduction of V^{4+} to V^{3+} has become the key to prepare $V^{3.5+}$ balanced electrolyte from pentavalent vanadium compounds such as V_2O_5.

The redox behavior of vanadium ions in different oxidation states is illustrated by reduction reactions as reflected by their standard electrode potentials (E_0). From the point of view of standard electrode potential, whether the reduction reaction from V^{4+} to V^{3+} in Eq. (4) can be carried out mainly depends on whether the oxidation potential of reducing agent is greater than the reduction potential by 0.34V[52]. As shown in Fig. 4, CH_3OH, HCOOH and $C_2H_2O_4$ show redox potentials lower than those of V^{4+}/V^{3+} pairs and $C_2H_2O_4$ (0.83V) > HCOOH (0.54V) > CH_3OH (0.32V).Thermodynamically, oxalic acid can further reduce V^{4+} to V^{3+}, but the reaction rate constant of V reduction by oxalic acid is very low and the energy barrier is very high, so the reaction is extremely slow, so the process of converting V^{4+} to V^{3+} is difficult to occur. Compared with formic acid, its oxidation potential provides sufficient thermodynamic driving force, and its more direct oxidation path and faster reaction kinetics enable it to effectively overcome the energy barrier and realize the reduction from V^{4+} to V^{3+}.

$$VO^{2+} + 2H^+ + e^- = V^{3+} + H_2O \qquad E_0 = 0.34\ V \qquad (4)$$

View Article Online
DOI: 10.1039/D5SU00532A

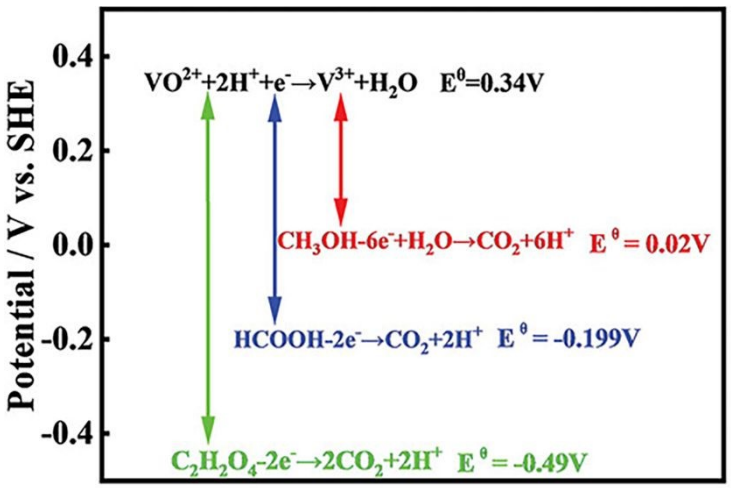

Fig. 4 Redox potential of V^{4+}/V^{3+}[52] (Reprinted with permission of MDPI)

2.4 Selection of vanadium raw materials

Vanadium is generally extracted from ores such as titanomagnetite[53] and stone coal mine through high-temperature roasting techniques[54, 55], which results in the production of V_2O_5, which is the main raw material for the preparation of electrolytes for VFB[56, 57]. Vanadium ore is roasted-acid leaching/alkali leaching-enrichment and precipitation of vanadium to produce crude ammonium metavanadate, and industrial ammonium metavanadate (purity 90-95%) is purified to over 99.5% by extraction, ion exchange resin and other processes to obtain high-purity ammonium metavanadate[58]. As a precursor of high-purity V_2O_5, the cost core of high-purity ammonium metavanadate lies in the taste of raw vanadium ore and waste and the accuracy of impurity control.

The preparation of $V^{3.5+}$ electrolyte mostly uses high-purity V_2O_5 as raw material to meet its purity and stability requirements, and its supply chain is mature and widely used. Using V_2O_5 as raw material, V^{5+} is firstly reduced to V^{4+} by chemical reduction-electrolysis method, and V^{4+} electrolyte is electrolyzed to 3.5 valence, or V_2O_5 slurry

View Article Online
DOI: 10.1039/D5SU00532A

is directly electrolyzed to 3.5 valence. At present, it has turned to a diversified raw material strategy. For instance, high-purity ammonium metavanadate can be used as a direct raw material to prepare $V^{3.5+}$ electrolyte by solid-phase reduction roasting and acid dissolution. And solvent extraction-electrolysis method with vanadium leaching solution or vanadium slag as raw materials.

As shown in Fig. (5a), the cyclic voltammetry (CV) curves of vanadium electrolytes prepared from high-purity V_2O_5 and impurity-containing $VOSO_4$ are basically the same, indicating that they have similar electrochemical activities. However, as can be seen from the impedance spectrum of Fig. (5b), the smaller impedance arc of V_2O_5 curve shows that the resistance of the electrolyte at the electrode interface is smaller and the reaction is faster, which is due to its extremely low impurity content, thus ensuring the performance of the electrolyte in long-term use[59]. This difference is mainly due to the extremely low impurity content of high-purity V_2O_5 raw materials, which significantly improves the interface performance and long-term operation stability of electrolyte. In practical application, high-purity V_2O_5 has been widely used in industrial scale because of its mature process and industrial chain. At present, the industrial supply of high-purity $VOSO_4$ is limited and the output is small. The above results also reflect the influence of raw material purity on the electrochemical performance of vanadium electrolyte.

View Article Online
DOI: 10.1039/D5SU00532A

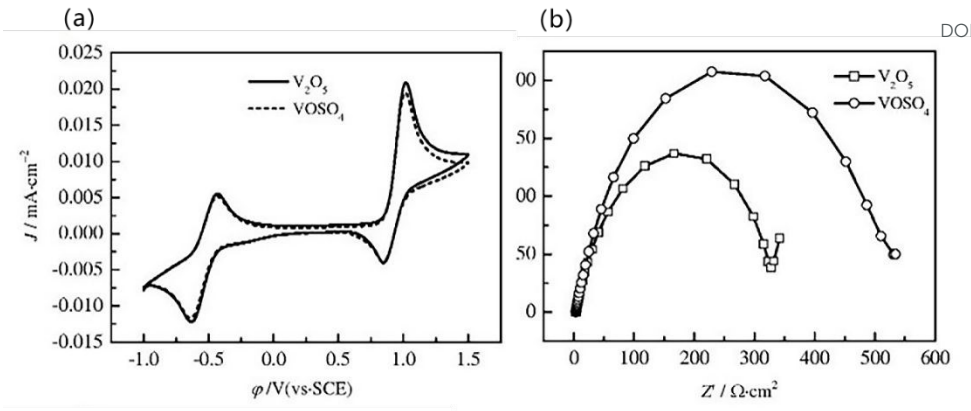

Fig. 5. (a) CV; (b) Impedance spectrum of V^{3+} electrolytes prepared with different raw materials[59](Reprinted with permission of MDPI)

3. Preparation methods of $V^{3.5+}$ electrolyte

The most direct preparation method of $V^{3.5+}$ electrolyte is to use high-purity $VOSO_4$ and $V_2(SO_4)_3$ or V_2O_3, V_2O_5, VCl_3 etc. as raw materials[60], mix them by valence ratio 3.5 and dissolve them in sulfuric acid or hydrochloric acid[61, 62]. However, the requirement of high purity of vanadium raw materials and poor solubility of vanadium oxides have made the acid dissolution method seldom used alone in practical applications. At present, the methods of preparing $V^{3.5+}$ electrolyte can be mainly divided into chemical reduction method, electrolysis method and chemical reduction-electrolysis method, among which chemical reduction-electrolysis method has become the mainstream method of industrial production of $V^{3.5+}$ electrolyte. The following is a detailed overview of its basic processes.

3.1 Chemical reduction method

3.1.1 Solid-phase reduction-acid dissolution method

The solid-phase reduction-acid dissolution is a method for preparing vanadium oxides by solid-phase reduction and then dissolving it in acid to obtain a $V^{3.5+}$

View Article Online
DOI: 10.1039/D5SU00532A

electrolyte[63, 64], in which the vanadium raw material provides the active substance of VFB, and the reducing agent regulates the valence of the vanadium electrolyte. To promote the reduction of vanadium from V^{4+} to V^{3+} oxidation state, it usually requires the use of strong reducing agents, such as hydrogen gas[65] and hydrazine hydrate at elevated temperatures.

Wu et al.[66] have developed a short-process ammonium salt vapor reduction method using ammonium metavanadate or poly-vanadate as vanadium sources presented in Fig. 6(a). Using V_2O_5 as raw material, under the conditions of reducing atmosphere of N_2:CO:H_2 = 80:17:3 and reacting at 700°C and 2h as shown Fig. 6(b) and Eq. (5-7). It is carried out by controlled reduction to generate mixed valence oxide containing VO_2 and V_2O_3. The V^{4+}/ V^{3+} ratio may not be exactly 1:1 due to process fluctuation, it is necessary to add high-purity V_2O_5 to adjust the valence state to 3.5. When V_2O_5 reacts with V^{3+} in acidic solution, a redox reaction occurs as shown in Eq. (8). V^{3+} acts as a chemical reducing agent that significantly accelerates the dissolution of V_2O_5, thereby mitigating its poor solubility. Although its solubility is low, the redox reaction will increase its solubility under the conditions of heating and stirring, and the valence state can be fine-tuned and stabilized by controlling its addition amount. Vanadium oxides have stable crystal structure, high lattice energy and generally poor solubility, most dissolution processes control acid concentration and reaction conditions according to the valence state of vanadium, such as temperature and pressure, or destroy the crystal lattice through the synergistic effect of acid dissolution and reduction.

View Article Online
DOI: 10.1039/D5SU00532A

$$(NH_4)_2V_6O_{16} = 6VO_2 + N_2 + 4H_2O \quad (5)$$

$$(NH_4)_2V_6O_{16} + 3CO = 3V_2O_3 + 3CO_2 + N_2 + 4H_2O \quad (6)$$

$$(NH_4)_2V_6O_{16} + 3H_2 = 3V_2O_3 + N_2 + 7H_2O \quad (7)$$

$$V_2O_5 + 2V^{3+} + 2H^+ = 4VO^{2+} + H_2O \quad (8)$$

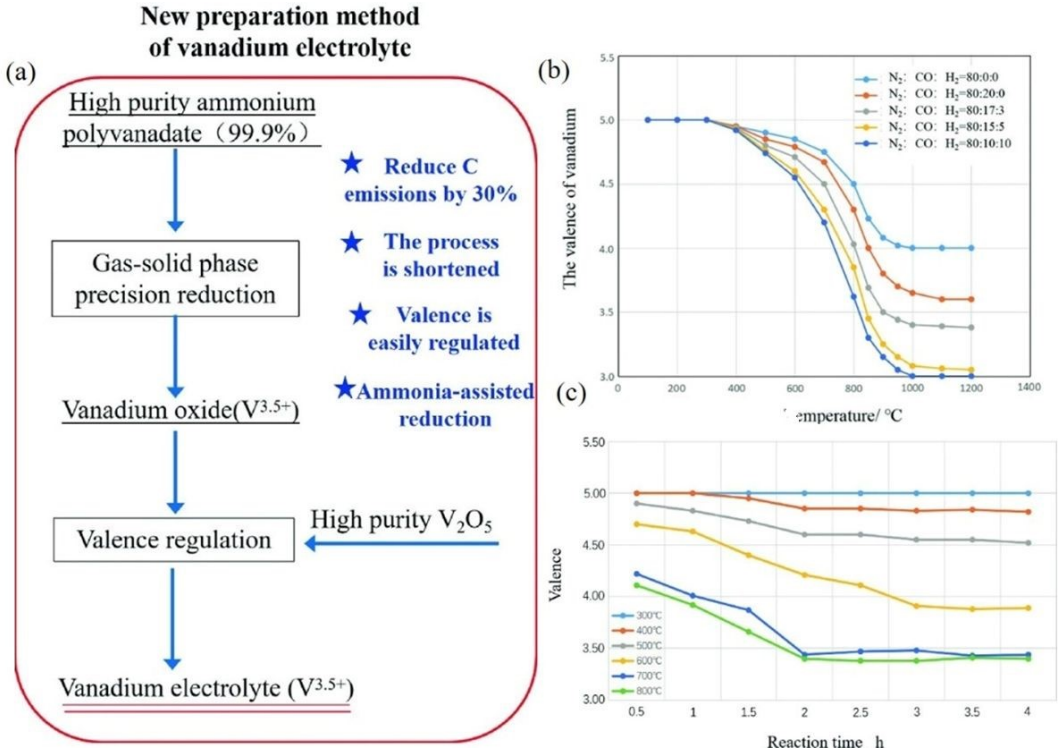

Fig. 6. (a) Process flow; The influence of (b) different reducing agent partial pressures; (c) temperature and reduction time[66](Reprinted with permission of Spinger Nature)

Du et al.[67] provided an approach for preparing $V^{3.5+}$ electrolyte with a short process. Using ammonia metavanadate as raw material and ammonia as reducing agent, the temperature is raised to 400-500℃ and when the temperature reaches the reaction temperature, ammonia gas is introduced for reduction reaction and the obtained roasted reduction product is acid-dissolved from the tube furnace to obtain vanadium electrolyte. The different valence states of vanadium in the reduction process are shown

View Article Online
DOI: 10.1039/D5SU00532A

in Fig. 7(a-c), and NH_4VO_3 in the raw material only contains V^{5+}. With the increase of reduction temperature, the concentration of V^{5+} gradually decreased and V^{4+} appeared and its concentration began to increase. At 350-400℃, the product began to transform from V^{4+} to V^{3+}. In the whole reduction process, the total average valence state of vanadium decreased in turn, indicating that the valence state of vanadium in the product was continuously reduced. In the reduction process as shown in Fig. 7(d), V_4O_7 can be obtained at 400-500℃. $V^{3.5+}$ electrolyte can be obtained after acid dissolution, it is found that increasing the reaction temperature, ammonia flow rate and prolonging the reaction time are conducive to the reduction process, this method provides a short process to prepare a $V^{3.5+}$ electrolyte.

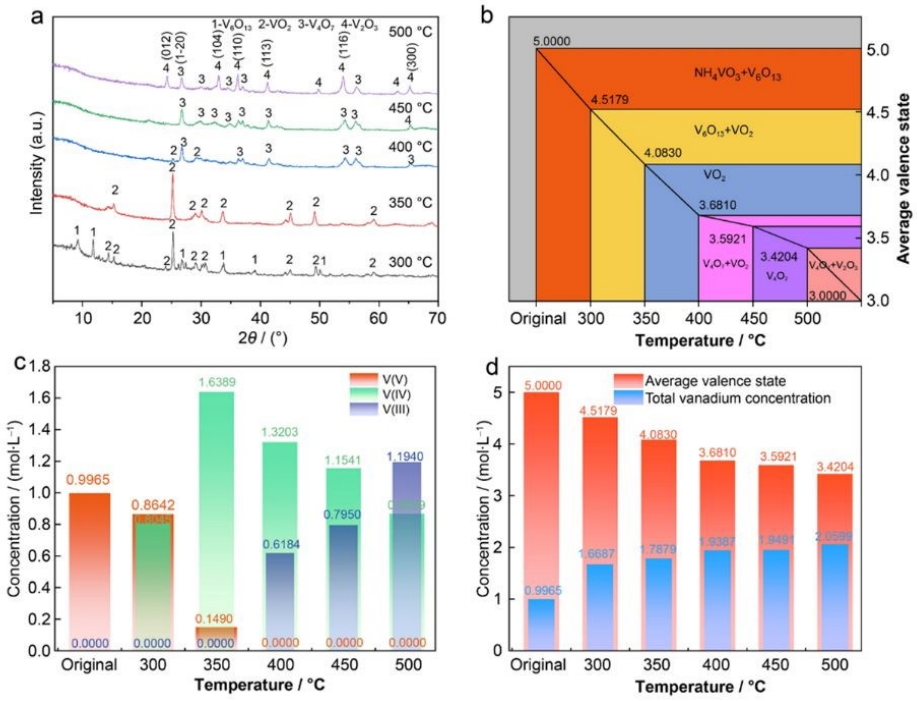

Fig. 7. With different temperatures: (a) XRD; (b) the average valence state and phase change; (c) the concentration of vanadium (d) the variation of total vanadium concentration and average valence state[67](Reprinted with permission of Spinger Nature)

View Article Online
DOI: 10.1039/D5SU00532A

In summary, solid-state reduction-acid dissolution method is used to prepare low-valent vanadium oxide through high-temperature reduction, and the acid dissolution of vanadium oxide is promoted through oxidation and reduction of V^{3+} and V^{5+}. The process flow is relatively simple, and the use of gases such as hydrogen can avoid the problem of reducing agent residue. However, it is necessary to accurately control the high-temperature reducing atmosphere, which involves flammable and explosive gases such as H_2, and has high energy consumption and high safety requirements for equipment.

3.1.2 Catalytic reduction method

Catalytic reduction method for the preparation of $V^{3.5+}$ electrolyte by chemical reduction under the action of catalysts, and the key to its application lies in the selection of catalysts and reducing agents. As the reducing agent of V^{4+} solution, methanol, formic acid and oxalic acid are usually chosen, which have lower cost, lower standard redox potential and the oxidation products are H_2O and CO_2 which are cleaner. In the choice of catalyst, Pt/C catalyst is widely used in the catalytic reduction due to its high activity. As for the reactors used, there are one-pot reactor, column reactor, fixed-bed reactor and fuel cell type reactor.

3.1.2.1 One-pot reactor

One-pot reactor is a relatively simple reaction mode. Under the temperature of 70 ℃ in N_2 atmosphere, V_2O_5, formic acid and Pt/C are mixed for hydrothermal reaction with formic acid as reducing agent and Pt/C as catalyst[16]. The process flow for the preparation of $V^{3.5+}$ electrolyte using V_2O_5 as the feedstock presented in Fig. 8, the

View Article Online
DOI: 10.1039/D5SU00532A

reaction equation is in Eq. (9):

$$V_2O_5 + 3/2HCOOH + 5H^+ = 2\ V^{3.5+}(VO^{2+} + V^{3+}) + 3/2CO_2 + 4H_2O \quad (9)$$

By analyzing the solution after catalytic reduction, the reduction effect and reaction process can be investigated. Potentiometric titration and Uv-vis methods are often used to determine the concentration of vanadium ions in acidic systems. If oxalic acid and formic acid are used as reducing agents, as shown in Fig. 9 (a-b), the UV-Vis spectrum is compared with the standard vanadium solution. It was found that the UV-Vis spectra of electrolyte solutions with different excess oxalic acid were almost the same as those of standard V^{4+} solution, and there was no characteristic V^{3+} peak, regardless of the existence of Pt/C catalyst. As shown in Fig. 9(c-d), V^{5+} was partially reduced to V^{4+}in different excess formic acid solutions. When Pt/C catalyst was introduced, a characteristic peak of V^{3+} appeared, and formic acid successfully reduced V^{5+} to $V^{3.5+}$. It was found that oxalic acid could not reduce V^{5+} to $V^{3.5+}$ even in the presence of the catalyst, but the use of formic acid could convert V^{5+} to $V^{3.5+}$. The oxidation state of the electrolyte was precisely controlled by adjusting the amount of formic acid, enabling the successful synthesis of $V^{3.5+}$ electrolytes.

View Article Online
DOI: 10.1039/D5SU00532A

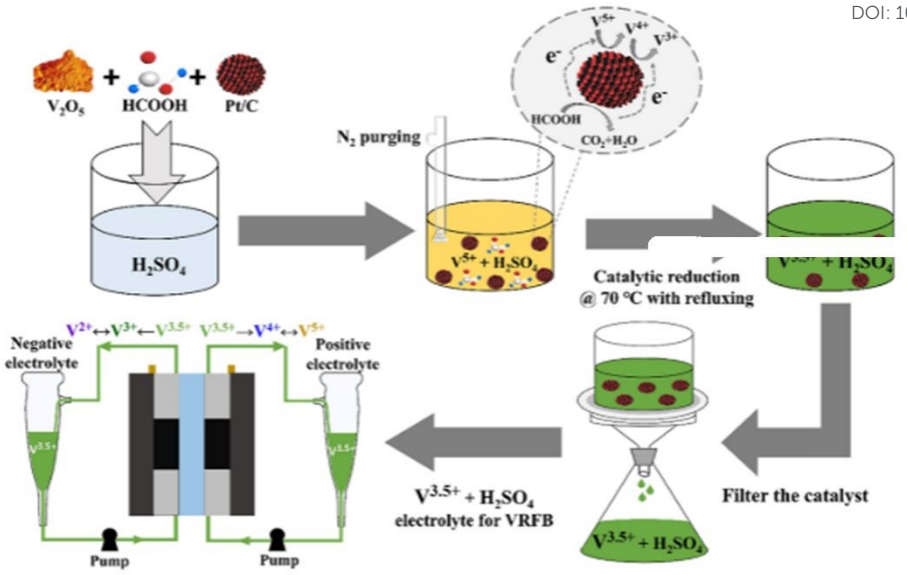

Fig. 8. Schematic of $V^{3.5+}$ electrolyte preparation using hydrothermal reduction[16] (Reprinted with permission of American Chemical Society)

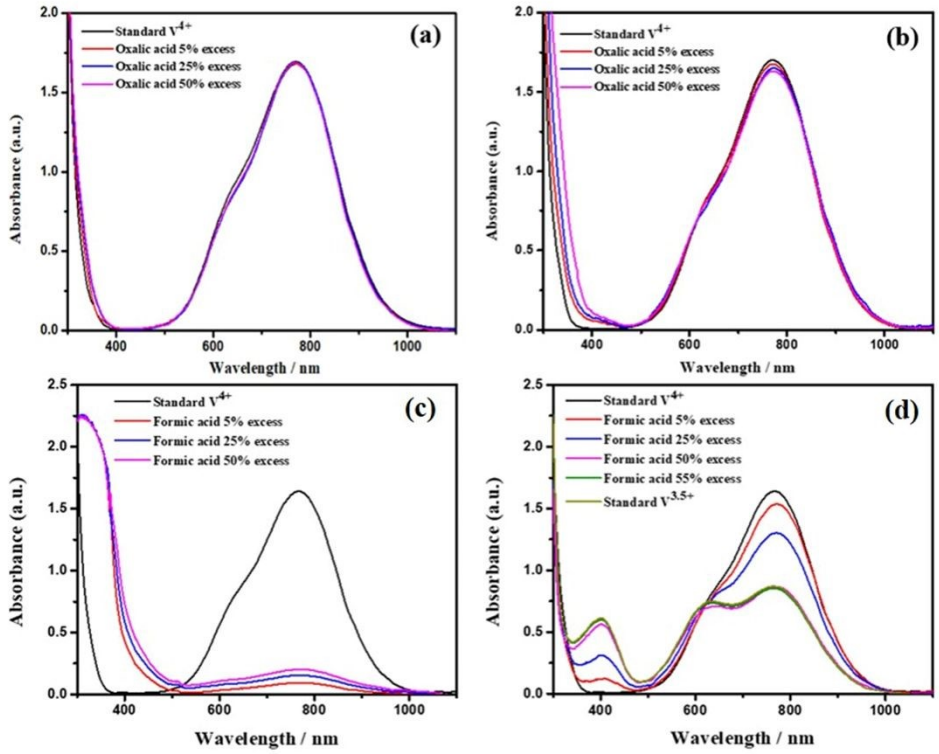

Fig. 9. UV–Vis spectra of the electrolyte with (a) oxalic acid;(b) oxalic acid in the presence of a Pt/C catalyst; (c) formic acid ;(d) formic acid in the presence of a Pt/C catalyst[16]. (Reprinted with permission of American Chemical Society)

View Article Online
DOI: 10.1039/D5SU00532A

3.1.2.2 Fixed bed reactor

The application of column-type hydrothermal reactor is available which is shown in Fig. 10, Xu et al.[68] proposed a method for the preparation of impurity-free $V^{3.5+}$ electrolyte by catalytic reduction using clean hydrogen, using the hydrothermal hydrogen reduction technique, and designed a Pt/C-modified graphite felt column-type catalytic reactor, with H_2 and $VOSO_4$ solution passed at the bottom of the reactor, and the $V^{3.5+}$ electrolyte was obtained at the top., the reaction equation is in Eq. (10):

$$2VOSO_4 + H_2 + H_2SO_4 = V_2(SO_4)_3 + 2H_2O \quad (10)$$

Comparing the electrochemical properties of $V^{3.5+}$ electrolyte prepared by electrolysis and catalytic hydrogen reduction, the CE and EE curves in Fig. 11(a-b) are basically the same, and the discharge capacity is 59.5% as shown in Fig. 11(c), showing similar capacity attenuation. Fig. 11(d) further shows that the charge and discharge curves of the two electrolytes are almost the same at the 1st, 50th and 100th cycles. These results confirm that the electrochemical performance of electrolyte produced by catalytic hydrogen reduction is consistent with that of conventional electrolysis and meets the quality standards required for application. The use of hydrogen as the reducing agent in this catalytic reaction is cleaner and has no impurity residue, and the use of Pt-based catalyst promotes the reduction of V^{4+} to V^{3+}, but this catalytic reactor requires a large amount of catalyst and has a high cost, and the use of hydrogen as the reducing agent also has transportation difficulties and safety hazards.

View Article Online
DOI: 10.1039/D5SU00532A

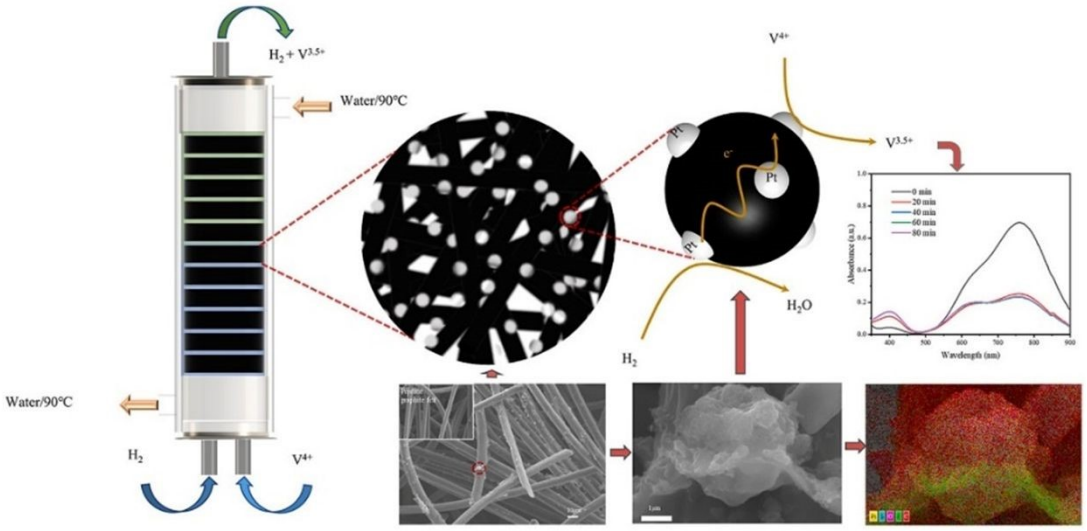

Fig. 10. Design model diagram of column reactor[68] (Reprinted with permission of Elsevier)

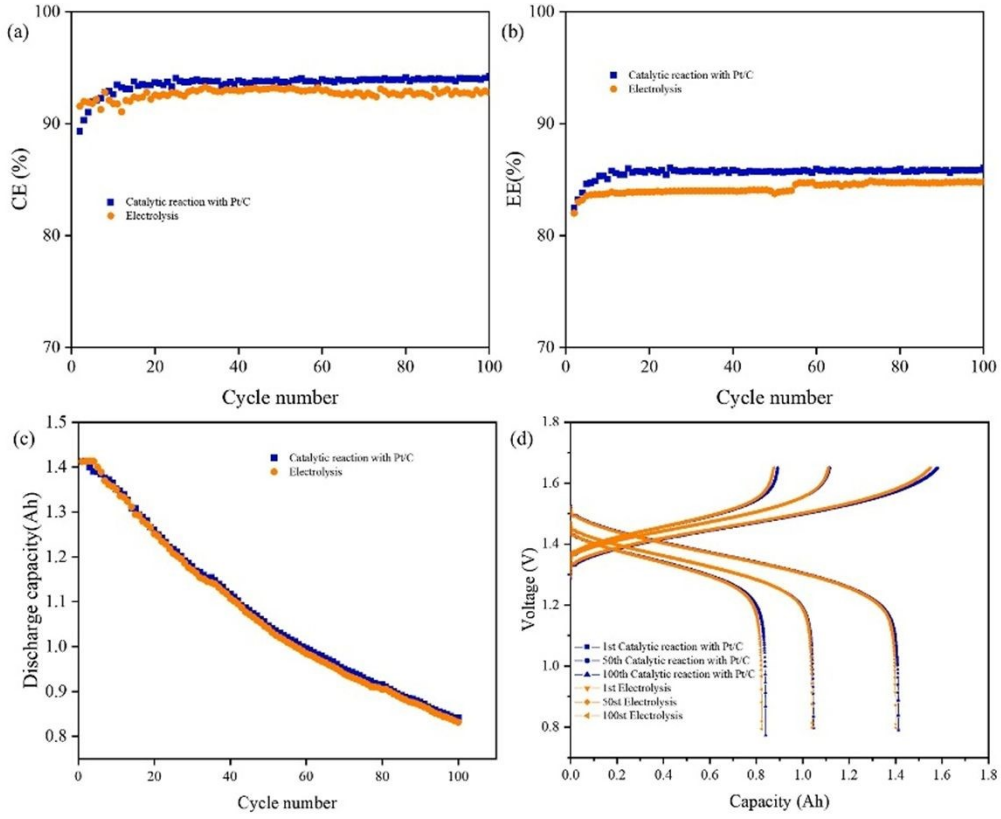

Fig. 11. (a) CE; (b) EE; (c) discharge capacities; (d) charge/discharge curves [69](Reprinted with permission of Elsevier)

Another typical examples of fixed-bed type are shown in Fig. 12 (a), HEO et al.[17]

View Article Online
DOI: 10.1039/D5SU00532A

d constructed a fixed-bed flow catalyst reactor by stacking Pt/C-modified carbon felts. After V^{4+} electrolyte and formic acid pass through the catalytic reactor, they are converted into $V^{3.5+}$ and generate CO_2 and H_2O under the catalysis of Pt/C on the reactor wall[36, 70]. As shown in the UV-Vis spectrum of Fig. 12(b), the absorbance at the characteristic peak of V^{4+} decreased at 760 nm, while the absorbance at the characteristic peak of V^{3+} increased at 401 nm, indicating the transformation from V^{4+} to V^{3+}. As shown in Fig. 12(c), the reaction can hardly occur without the catalysis of Pt/C, and the reaction conversion rate increases with the increase of temperature at 50-80°C, which shows that the existence of Pt/C and certain temperature conditions are essential for the chemical production of $V^{3.5+}$. It is very important to reduce the activation energy of formic acid oxidation, which proves the feasibility of continuous electrolyte production.

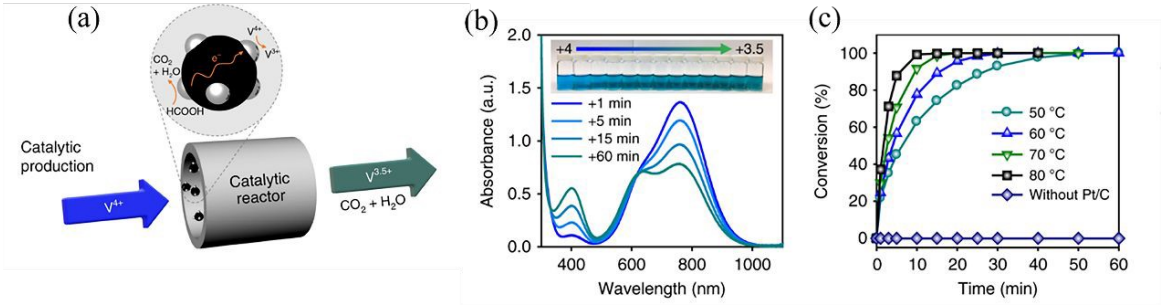

Fig. 12. (a) Reactor with fixed-bed Pt/C catalysts; (b)UV–Vis spectra of the reactant electrolyte at different reaction times at 50°C; (c) Conversion diagram with and without Pt/C at 80°C[17](Reprinted with permission of MDPI)

3.1.2.3 Fuel cell type reactor

As shown in Fig. 13(a), Sun et al.[52]constructed a bifunctional liquid fuel cell by using formic acid as an anodic fuel and V^{4+} ions as a cathodic oxidant. The anodic

View Article Online
DOI: 10.1039/D5SU00532A

formic acid decomposed into CO_2 and H_2O and the cathodic V^{4+} was reduced to $V^{3.5+}$. The valence state of electrolyte before and after the reaction was measured by UV-Vis spectrum in Fig. 13(b), and there was only one characteristic absorption peak of V^{4+} at 760 nm, while an additional absorption peak of V^{3+} appeared at 610 nm after the reaction, which indicated that the fuel cell could achieve V^{4+} reduction. The reaction mode of fuel cell opens a new pathway for the preparation of $V^{3.5+}$ electrolyte.

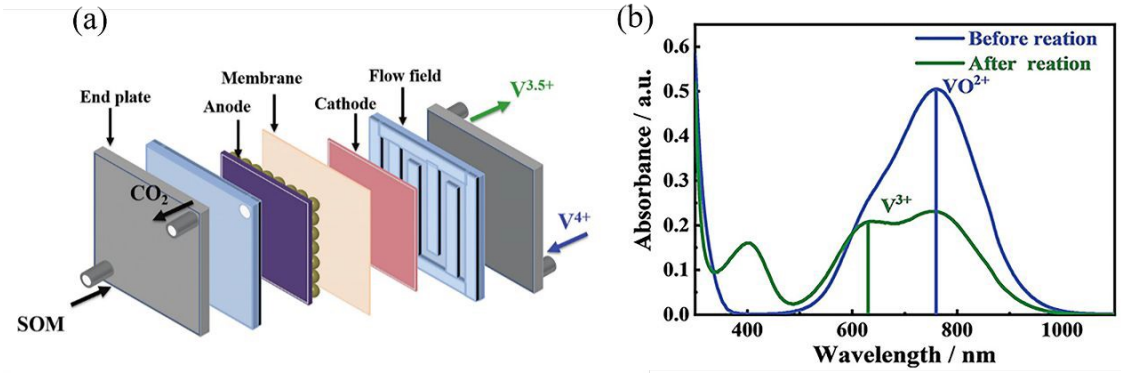

Fig. 13. (a) Schematic diagram and reaction mechanism of fuel cell reactor; (b) UV–vis spectra of the electrolytes before and after reaction[52] (Reprinted with permission of MDPI)

The selection of catalysts and reducing agents in catalytic reduction methods is extremely crucial. In addition to formic acid, ascorbic acid, oxalic acid and other available organic reductants, the key is to find the reductants with clean products, strong reducing ability, low cost and more applicability. The use of platinum catalyst increases the production cost of the electrolyte, and there has not yet appeared a product that can replace the Pt/C catalyst, so it is necessary to develop new catalysts that can both improve the catalytic reaction speed and reduce the amount of platinum. It has been studied to improve the durability and high efficiency of catalytic materials by means of

View Article Online
DOI: 10.1039/D5SU00532A

improving Pt/C catalysts, such as doping metal elements and adjusting the electronic structure between materials, etc. The performance of the improved catalysts has been improved to a certain extent, and there are also some problems in practical applications.

3.2 Electrolysis method

3.2.1 Oxygen evolution electrolysis

Oxygen evolution electrolysis usually employs an electro-stack and its structure is [71] shown in Fig. 14. The electrolysis system is designed with a continuous-flow electro-stack structure for with a perfluoro-sulfonic acid membrane as the separator, graphite plates as cathodes, and titanium plates or titanium-based coated electrodes as anodes, ruthenium-iridium (Ru-Ir) and iridium-tantalum (Ta-Ir) coatings exhibit excellent electrocatalytic activity and superior corrosion resistance. During the electrolysis process, a V_2O_5 sulfuric acid solution or $VOSO_4$ solution is introduced into the cathode, and the V^{5+} or V^{4+} is reduced as shown in Eq. (11-12). A sulfuric acid aqueous solution is electrolyzed with oxygen being generated at the anode as shown in Eq. (13)[72]. The electrochemical reaction and ion migration occurred in the battery driven by external electric energy, and finally the electric energy was converted into chemical energy for storage, as shown in Fig. 15. The anode produces O_2 and H^+, which drives the cathode to reduce V^{5+}/V^{4+} to $V^{3.5+}/V^{3+}$, and H^+ migrates through the membrane to complete the current loop. The reaction of the whole process is shown in Eq. (14-15).

Cathode：

$$VO_2^+ + e^- + 2H^+ = VO^{2+} + H_2O \quad (11)$$

$$VO^{2+} + e^- + 2H^+ = V^{3+} + H_2O \quad (12)$$

View Article Online
DOI: 10.1039/D5SU00532A

Anode： $2H_2O - 4e^- = 4H^+ + O_2\uparrow$ (13)

Overall：

$V_2O_5 + 3H_2SO_4 = V_2(SO_4)_3 + 3H_2O + O_2\uparrow$ (14)

$4VOSO_4 + 2H_2SO_4 = 2V_2(SO_4)_3 + 2H_2O + O_2\uparrow$ (15)

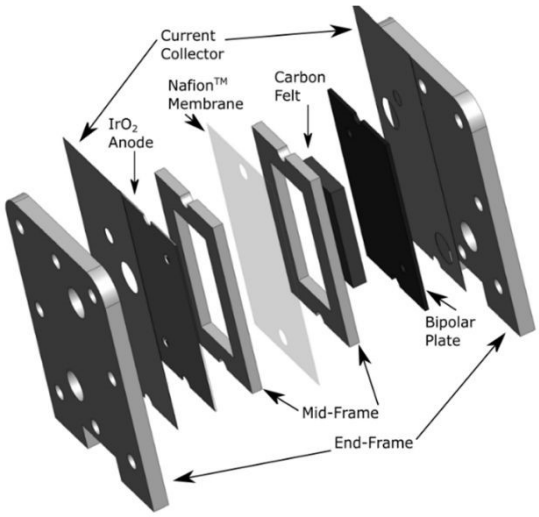

Fig. 14. Schematic diagram of battery structure used in oxygen evolution electrolysis[73] (Reprinted with permission of John Wiley and Sons)

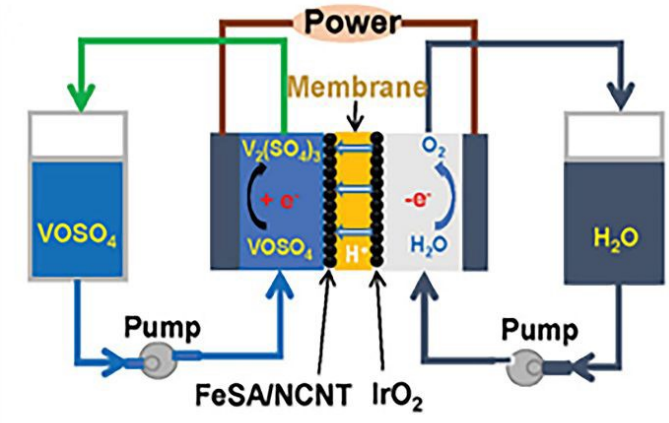

Fig. 15 Schematic of the oxygen evolution electrolysis[74] (Reprinted with permission of John Wiley and Sons)

As shown in Fig. 16, high-purity V_2O_5 powder, 4 to 5mol/L sulfuric acid solution, and water are fed into the reaction vessel in specific proportions. Under stirring and

View Article Online
DOI: 10.1039/D5SU00532A

heating conditions to form an acidic slurry[73]. This slurry is then passed through a filtration unit to remove undissolved particles and impurities, yielding a clear solution. This solution undergoes a reduction reaction at the cathode of the electrolysis cell, and the resulting V^{3+} ions are circulated back to the reaction vessel. As indicated in Eq (8), V^{3+} acts as a chemical reducing agent that significantly accelerates the dissolution of V_2O_5, thereby mitigating its poor solubility. This method requires high-purity raw materials, impurities may contaminate the electrolyte. Additionally, the highly acidic environment necessitates corrosion protection measures for the equipment.

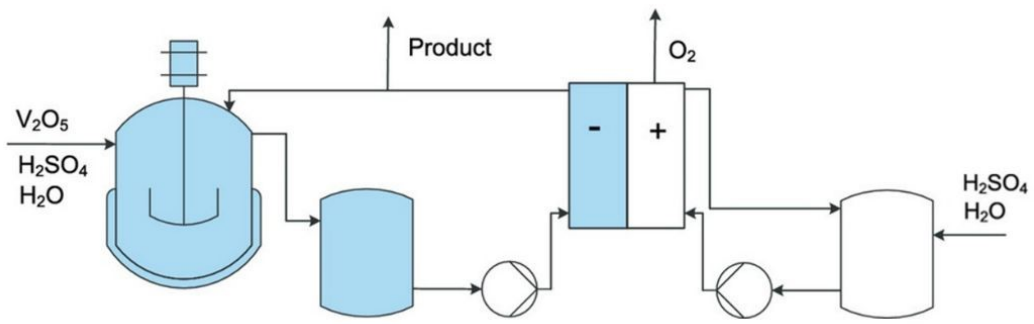

Fig. 16. Process flow for production of vanadium electrolyte[73] (Reprinted with permission of John Wiley and Sons)

The modular design of stack structure by oxygen evolution electrolysis can highlight the integration advantages and allow it to operate at relatively high voltage, which is conducive to shorten the reaction time, enhancing system adaptability and realizing large-scale continuous production[75]. Although the stack structure has brought the advantages of efficiency and adaptability, with strict equipment requirements and technical threshold, anode noble metal catalysts such as Ir and Ru are expensive and scarce, and the cost of corrosion-resistant materials and ion exchange membranes is

View Article Online
DOI: 10.1039/D5SU00532A

also high. The initial investment of the whole electrolysis system is large, and the system needs to operate under the conditions of strong acid and high potential, which puts forward extremely high requirements for the sealing, durability and daily maintenance of the equipment.

3.2.2 VFB electrolysis

The VFB electrolysis method involves injecting a V^{4+} electrolyte into the both the cathode and anode electrodes of VFB, with the cathode electrode obtaining a $V^{3.5+}$ or V^{3+}, whereas the anode electrode portion requires the addition of an additional reducing agent to lower the vanadium valence[76]. The reactions involved in the electrolysis-chemical reduction process are by the Eq. (16-18), the anode electrolyte usually needs to add oxalate reducing agent to get V^{4+} by the Eq. (19):

Cathode: $VO^{2+} + e^- + 2H^+ = V^{3+} + H_2O$ (16)

Anode: $VO^{2+} - e^- + H_2O = VO_2^+ + 2H^+$ (17)

Overall: $2VO^{2+} = VO_2^+ + V^{3+}$ (18)

Chemical reduction: $VO_2^+ + C_2O_4^{2-} + 4H^+ = 2CO_2 + VO^{2+} + 2H_2O$ (19)

During the above process, the cathode and anode electrocatalytic electrodes are composed of one or more materials selected from C-based substrates. The C-based materials encompass graphitized/non-graphitized plates, porous carbon felt, carbon paper, or porous carbon plates, with pore diameters ranging between 1 and 200 μm. The battery electro-stack utilized in the VFB electrolysis method demonstrates significant structural and operational variations compared to the oxygen evolution electrolysis with detailed comparisons provided in Table 3.

View Article Online
DOI: 10.1039/D5SU00532A

Table 3 Comparison of the oxygen evolution electrolysis and VFB electrolysis method

	Oxygen evolution electrolysis	VFB electrolysis
Anode material	Ti plate with Ru-Ir or Ir-Ta coatings	C-based substrates
Voltage	About 5V	1~1.6V
Anode electrolyte	H_2SO_4 solution	V^{4+} electrolyte
Cathode electrolyte	V^{5+}/V^{4+} electrolyte	V^{4+} electrolyte
Anode reaction	$H_2O \rightarrow O_2$	$V^{4+} \rightarrow V^{4.5+}$
Cathode reaction	$V^{5+}/V^{4+} \rightarrow V^{3.5+}$	$V^{4+} \rightarrow V^{3.5+}$

The process of oxygen evolution electrolysis is short and it can consumes less time, which is commonly used in industry[77, 78]. However, it requires high working voltage and high energy consumption, and relies on Ir/Ru-based noble metal catalyst. The acidic oxygen evolution reaction accelerates electrode corrosion, which affects the durability of equipment and increases the cost of long-term operation. The operating voltage and energy consumption of VFB electrolysis are low, and the electrolysis conditions are relatively mild. Carbon-based materials are mostly used, the system is simple and convenient to maintain and the relatively mild operating environment is conducive to long-term operation. However, the introduction of reducing agent is complicated, which easily leads to the residue of impurities and affects the performance of electrolyte.

View Article Online
DOI: 10.1039/D5SU00532A

3.3 Chemical reduction-electrolysis method

The chemical reduction-electrolysis method is predominantly employed in industry, wherein V^{4+} electrolyte prepared from V^{5+} sources by chemical reduction necessitates supplementary electrolysis for the preparation of $V^{3.5+}$ electrolyte[21, 79].

3.3.1 Reduction of V_2O_5 in H_2SO_4 solution followed by electrolysis

At present, the commonly used method in industry is to reduce high-purity V_2O_5 (purity greater than 99.5%) with oxalic acid as reducing agent to obtain sulfuric acid solution of $VOSO_4$. The resulting solution was incorporated into the VFB and charged through oxygen evolution electrolysis or VFB electrolysis to prepare $V^{3.5+}$ electrolyte. The reaction of reducing V_2O_5 to V^{4+} by oxalic acid has the advantage of low temperature requirement and no need of high pressure. The heat of exothermic and redox reaction can be diluted by sulfuric acid to reach the temperature of rapid and complete reaction. Yang et al.[80] reduced V_2O_5 to prepare electrolytes utilizing reducing agents like oxalic acid, ascorbic acid, tartaric acid, citric acid, hydrogen peroxide, formic acid, and acetic acid. The preparation conditions of oxalic acid reduction to prepare electrolyte are reaction temperature 90℃ and reaction time 100min, the conversion rate of V^{5+} to V^{4+} reaches 94.8%.

The preparation of high-purity V_2O_5 is a key link because vanadium electrolyte has high requirements on impurity elements. In addition to using V_2O_5, related investigations[81] have adopted Na_3VO_4 solution as raw material, calcium vanadate solid was prepared by chemical precipitation, and V^{5+} was reduced to V^{4+} by oxalic acids under strong acidic conditions to generate $VOSO_4$ solution. Calcium ions and sulfate

View Article Online
DOI: 10.1039/D5SU00532A

ions formed calcium sulfate precipitation to remove it, and finally $V^{3.5+}$ electrolyte was obtained by electrolytic purification. This method uses precipitation method to remove calcium ion impurities, which expands the selection range of raw materials, but the operation steps are complicated.

3.3.2 Solvent extraction of V(IV) followed by electrolysis

Due to the long preparation process, heavy pollution and low vanadium yield of high-purity V_2O_5 as raw material[82], the preparation cost of electrolyte is high. Therefore, purifying the intermediate or primary product of vanadium extraction in metallurgical process to prepare vanadium electrolyte can shorten the process flow and reduce the production cost. The Institute of Process Engineering of China Academy of Sciences, where the author is affiliated, put forward the method of extracting and purifying V^{4+} solution by solvent extraction to prepare $VOSO_4$ vanadium electrolyte[83] and then electrolyzing to prepare $V^{3.5+}$ electrolyte.

As shown in Fig. 17, the leach solution of sodium-roasted vanadium slag is used as raw material, and sulfuric acid and a lower-priced reducing agent such as sodium sulfite are added to obtain crude tetravalent vanadium solution[84]. After extraction with acidic phosphine extractant and scrubbing, V(IV) was selectively extracted, and impurities such as Cr, Al, Fe, Si, Ca, Cl and Na in the solution were effectively separated. After stripping with H2SO4 solution, the high-purity $VOSO_4$ electrolyte was obtained, which was treated by electrolysis to obtain $V^{3.5+}$ electrolyte. One kind of the structures of the fresh extractant and vanadium-loaded extractants is shown in Fig. 18. The main reactions that occurred during the extraction process are represented as Eq.

View Article Online
DOI: 10.1039/D5SU00532A

(20-21).

$$VO^{2+}_{(aq)} + 2(HA)_{2(org)} = VOA_2\,HA_{(org)} + 2H^{+}_{(aq)} + HA_{(org)} \quad (20)$$

$$VO^{2+}_{(aq)} + 2(HA)_{2(org)} = VOA_2\,(HA)_{2(org)} + 2H^{+}_{(aq)} \quad (21)$$

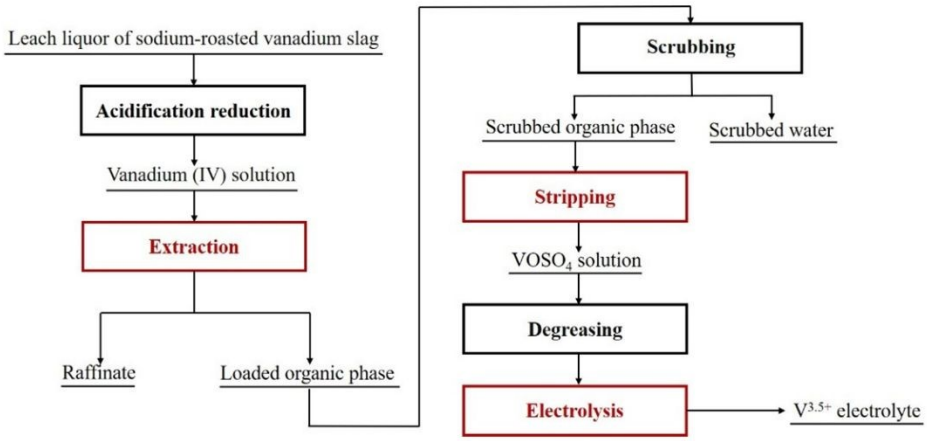

Fig. 17. Flow diagram for preparing $V^{3.5+}$ electrolyte by the solvent extraction

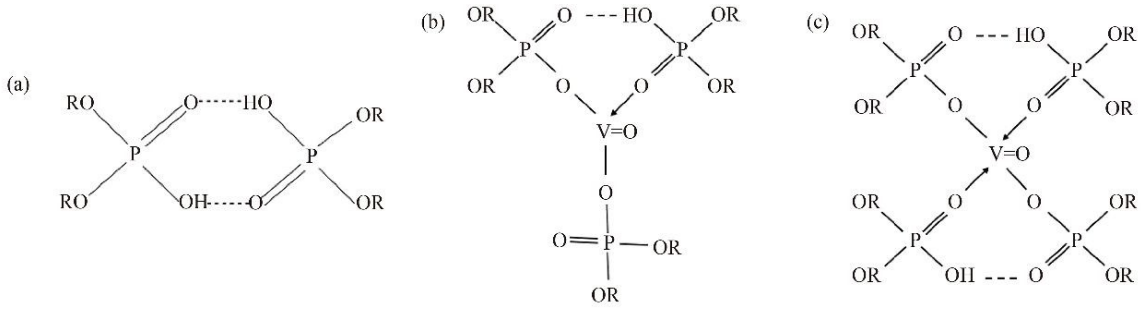

Fig. 18. (a) Dimer structure of D2EHPA extractant in organic phase;(b-c) VO^{2+} ions coordinate with multiple D2EHPA monomolecular in the loaded organic phase[85] (Reprinted with permission of Springer Nature)

The whole process of the method is based on a liquid-liquid reaction separation system, which simplifies the production process, omits solid-liquid conversion processes such as preparation and dissolution of V_2O_5 in the traditional process, can get rid of dependence on high-purity vanadium raw materials, reduces the production cost, and has the advantages of shortening time and saving energy, and the extraction

View Article Online
DOI: 10.1039/D5SU00532A

operation can realize continuous and automatic production with relatively high efficiency. Besides, the complexation between SO_4^{2-} and Cr(III) under higher SO4 concentrations in this system, inhibiting the extraction of chromium, thus enhancing the separation of vanadium and chromium, and high-purity vanadium electrolyte with vanadium, chromium and sulfuric acid concentrations of 2.12 mol/L, 0.11 mg/L and 1.75 mol/L was prepared[86]. The prepared high-purity $VOSO_4$ electrolyte was de-oilded by resin or activated carbon, followed by further electrolysis to produce high-purity $V^{3.5+}$ electrolyte. At present, our research group has expanded the raw materials of this process to the leaching solution of stone coal, industrial crude ammonium metavanadate and ammonium poly-vanadate.

Up to now, solvent extraction of V(IV) with acidic phosphorus extractants such as P204 and P507 followed by electrolysis to prepare $V^{3.5+}$ electrolyte has become a research hotspot in this field. In the recent related research, the raw solutions used in the extraction process involve vanadium slag calcified roasting reduction acid leaching solution[87], stone coal acid leaching solution[88], vanadium-rich solution after stone coal extraction and purification[89], high chlorine stone coal leaching solution[90], vanadium precipitation wastewater[91] and so on. Some improved method involves using EDTA to complex ferric iron to inhibit iron extraction[92], utilizing an H_2O_2-NaClO efficient selective oxidative stripping system within the D2EHPA extraction process, etc. Besides, tri-octyl ammonium chloride (N263) extractant is also used in the preparation of vanadium electrolysis. With vanadium slag as raw material, sodium diethyldithiocarbamate (DDTC) is used to complex V^{4+} ions in vanadium solution,

View Article Online
DOI: 10.1039/D5SU00532A

which is recovered in the form of calcium salt CaV_2O_5, then leached with carbonic acid and extracted with N263[93], $VOSO_4$ electrolyte similar to commercial high-purity $VOSO_4$ is successfully prepared. Naseer, M. U. H. et al.[88] prepared vanadium sulfate electrolyte from the acid leaching solution of stone coal using a solvent extraction-complexation reduction- stripping method. As shown in Fig. 19, VO^{2+} ions are first oxidized by H_2O_2 form pentavalent $VO(O_2)_2^-$, followed by solvent extraction of vanadium using N263; An H_2SO_4 solution mixed with oxalic acid is used as the stripping solution, realizing the direct reduction and stripping of V^{5+} back to the V^{4+}, ultimately yielding a $VOSO_4$ solution. The standard electrolyte sample (SS) was synthesized using high-purity $VOSO_4$ crystal with both vanadium ion concentration and sulfuric acid concentration specifically same as the electrolyte prepared through solvent extraction methodology (ES)[91]. Seen from the CV curve in Fig. 20 (a) the anode peak current density (jpa) obtained by SS is 84.18 mA cm^{-2} while that of ES is 77.91 mA cm^{-2}, and the jpa/jpc values are almost the same. The voltage change in the first charge-discharge cycle is shown in Fig. 20(b), the voltage efficiency (VE), energy efficiency (EE) and CE of ES and SS are shown in Fig. 20(c), in which CE and EE of ES are close to 90% of SS.

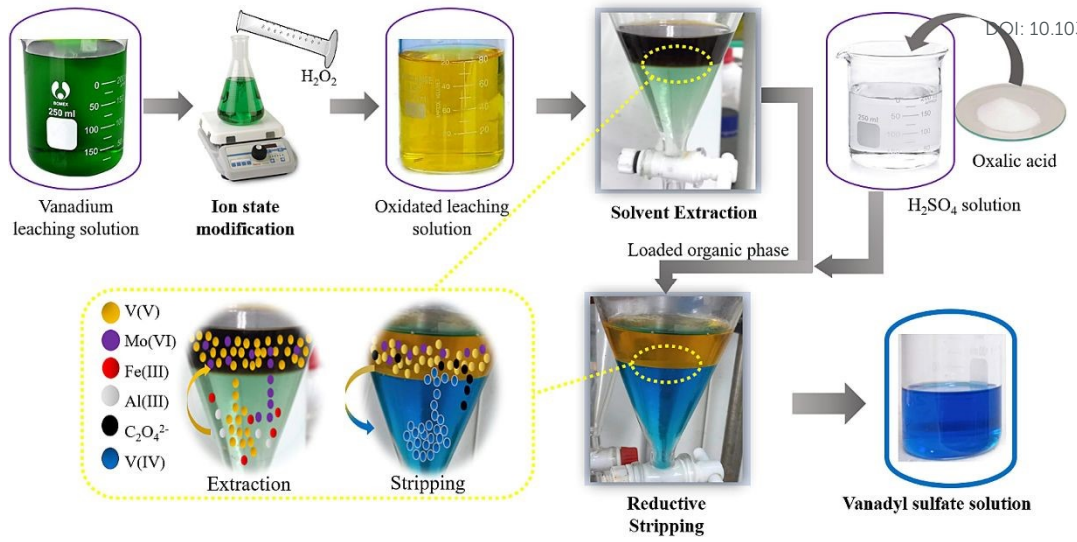

Fig. 19 Flow diagram of a solvent extraction-complexation reduction- stripping method[88] (Reprinted with permission of Elsevier)

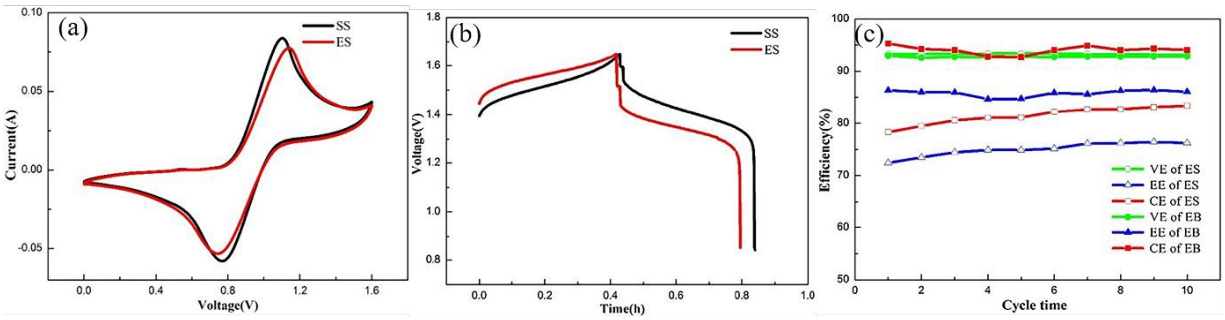

Fig. 20 (a) CV curves; (b) voltage change;(c) the efficiency of SS and ES[94] (Reprinted with permission of Elsevier).

The above data show that the performance of electrolyte prepared by solvent extraction, and the charging and discharging characteristics are highly similar the standard vanadium electrolyte, indicating that solvent extraction is a promising process. During the extraction process, trace amounts of oil at ppm levels inevitably contaminate the V^{4+} electrolyte due to solvent-solution contact. While the operational impact of such oil residues on VFB remains undetermined, current purification techniques, utilizing resin or activated carbon adsorption to reduce oil content below 0.1 ppm, thereby mitigating potential adverse effects on VFB performance. How to improve the

View Article Online
DOI: 10.1039/D5SU00532A

selectivity of extractant and unoil the stripping liquid to avoid impurities from entering the product is a key problem that needs to be paid attention to in this method.

Compared with single chemical reduction method and electrolysis method, chemical reduction-electrolysis technology is mature, and the process is more widely used. The addition of raw materials and reducing agents should be accurately controlled to ensure the purity and quality of electrolyte. The comprehensive application conditions of the two typical processes are shown in the following Table 4.

Table 4 Comprehensive comparison of two chemical reduction-electrolysis method

	Reduction of V_2O_5 in H_2SO_4 solution	Solvent extraction of V(IV)
Raw material requirements	High-purity V_2O_5 (≥98%)	Vanadium leaching solution
Technological process	Dissolution → reduction → filtration → electrolysis	Pre-impurity removal → extraction → stripping → electrolysis
Cost of production	Long process, high energy consumption and high wastewater treatment cost	Short process and low energy consumption
Product purity	Easily residual oxalic acid impurities	The impurity content is low (Na≤10 mg/L, Cr≤5 mg/L)
Technical maturity	Industrial application	Extensive industrial application demonstration stage

View Article Online
DOI: 10.1039/D5SU00532A

Environmental impact	Acid-containing wastewater and oxalic acid residue have high treatment cost	No ammonia nitrogen emission, recyclable solvent and clean production.

3.4 Sustainability analysis of preparation technology

Table 5 is a comprehensive evaluation of the sustainable development ability of several typical methods, including the selection of raw materials, energy consumption, production of three wastes and economic principles. In the above process, the process parameters in the industry are estimated by combining with the general database, and the estimated electrolyte energy consumption of each comparative process is obtained for comparative analysis[82].

For example, to calculate the energy consumption of preparing an electrolyte with a concentration of 1.6 mol/L $V^{3.5+}$ electrolyte by oxalic acid reduction V_2O_5 combined with electrolysis, the quantities of V_2O_5, $H_2C_2O_4$ and H_2SO_4 needed to produce $1m^3$ electrolyte are calculated according to the chemical reaction equation, and the energy consumption of raw material production is estimated by querying the database (LCA). According to the reaction equation, reducing 1.6 kmol of vanadium requires 0.8 kmol of oxalic acid, and the energy consumption for producing oxalic acid is about 25 MJ/kg, and the implied energy consumption is 1.80 GJ. The reactants are heated to the reaction temperature of 85℃ and maintained for several hours. According to the reaction temperature and holding time, the heat required for heating is calculated by the average specific heat capacity of materials and the amount of materials used, and the total heat consumption is estimated by considering the energy consumption of electrolyte concentration and the heat loss efficiency of reaction as shown in Eq. (22).Assuming

View Article Online
DOI: 10.1039/D5SU00532A

that the total mass of the system is about 1200 kg, mainly water and sulfuric acid, the average specific heat capacity C_P about4.0 kJ/(kg · k) and the thermal efficiency η about 80%, the calculated sensible heat required for heating is about 7.5-9.0 GJ/m. Estimate the power and running time of dasher, electrolytic equipment, etc., and calculate the amount of charge required to produce unit volume electrolyte according to Faraday's Law to calculate energy consumption. The theoretical charge Q required for reducing 0.8 kmol V^{4+} is calculated, the cell voltage is 0.5V, the current efficiency is 90%, and the calculated power consumption is 35.74kwh, which is converted into 0.129 GJ. The power consumption of pumps and control systems accounts for about 20% of the main power consumption, the total energy consumption of electrolysis section is 0.155 GJ, and the total energy consumption is 10.455GJ/m^3. The estimated range is 9-11 GJ.

$$E_{total}=E_{ele}+E_{th}+\sum(m_i\times EE_i) = \sum Pt+\sum cm\Delta t+\sum(m_i\times EE_i) \quad (22)$$

E_{total} represents the total energy consumption of the preparation process (GJ/m^3); E_{ele} represents the total power consumption in preparation process (kWh); E_{th} represents the total heat consumption (GJ) during preparation; m_i represents the consumption mass of the chemical i(kg); EE_i represents the embodied energy (GJ/kg) of the chemical i.

Table5 Evaluation of sustainable development ability of typical preparation methods of $V^{3.5+}$ electrolyte[82]

	Acid dissolution	Reduction roasting-acid dissolution	Electrolysis	Catalytic reduction	Chemical reduction-electrolysis

View Article Online
DOI: 10.1039/D5SU00532A

Raw material	V_2O_5/V_2O_3	V_2O_5/Vanadate	$V_2O_5/VOSO_4$	$V_2O_5/VOSO_4$	Leaching Solution/ Wastewater
Energy consumption	14-17GJ/m^3	15-18GJ/m^3	9-12 GJ/m^3	10-13 GJ/m^3	9-11 GJ/m^3
Three-wastes discharge	Acid waste water	Ammonia-nitrogen wastewater	Low hazardous waste	Catalyst residue treatment needed	CO_2 waste gas and solid waste
Economic viability	High-purity raw materials are difficult to obtain	Safety equipment for investment is high	Depends on the electricity price.	Catalyst cost is high.	The cost is relatively low.

4 Capacity recovery strategy of Vanadium electrolyte

4.1 Capacity fading

During the long-term operation of VFB, with the charge and discharge process, H^+ ion migrates at the anode and cathode. Due to the limited vanadium resistance of ion exchange membrane, vanadium ions and water molecules will also migrate through the membrane under the action of electric field and osmotic pressure[95-97]. For example, driven by concentration gradient, V^{2+} ion migration diffuses from the negative electrode through the ion exchange membrane to the positive electrode, resulting in the decrease of the volume of the negative electrode electrolyte and the total amount of vanadium ions, and the accumulation of vanadium ions in the positive electrode electrolyte, resulting in concentration imbalance. When V^{2+} migrates to the positive electrode, it will have a self-discharge reaction with high valence vanadium ions in the positive

View Article Online
DOI: 10.1039/D5SU00532A

electrode, consuming electrons that can be used for normal charging and discharging, and making the average valence state of the electrolyte of the positive and negative electrodes deviate from 3.5 valence, and the valence state of the electrolyte is further unbalanced[98].

In view of this capacity decay process, the related study[99] that actively improves the initial average valence state of electrolyte and generate excessive VO_2^+ in the first charge-discharge cycle to inhibit the accumulation and migration of V^{2+} in the cycle process, although this strategy will lead to the decrease of the actual available capacity in the first dozens of cycles, which really improves the stability and cumulative output capacity of the battery from the whole life cycle. The contact of oxygen in the air with the negative electrolyte leads to the increase of the valence state of the electrolyte, and the occurrence of side reactions such as hydrogen evolution and oxygen evolution, which leads to the vanadium ions in the positive and negative electrolyte being mainly V^{5+} and V^{3+}, and the battery with unbalanced valence state between the positive and negative electrodes cannot be charged and discharged[100-102]. Most of the capacity loss can be recovered by mixing two kinds of half-cell electrolytes periodically, but the capacity loss caused by hydrogen evolution reaction and air oxidation needs electrochemical or chemical rebalancing[103]. In addition to the above means of volume and valence recovery, there are also more studies on electrochemical system equipment, membrane improvement, etc., dedicated to alleviate the decline in battery capacity from multiple perspectives[104-106].

4.2 Capacity recovery

View Article Online
DOI: 10.1039/D5SU00532A

4.2.1 Positive and negative electrolytes mixing

The mixing of electrolytes can significantly extend the cycle life by restoring part of the capacity loss caused by the asymmetric transfer of various charged vanadium ions[107]. As shown in Fig. 21, when the volume deviation between the cathode and anode electrolytes reaches a certain extent, the electrolyte at the higher level is pumped by means of a transfer pump, an overflow pipe or a connecting pipe, etc. to the electrolyte at the lower level to balance the concentration of vanadium ions in each electrolyte[100, 105].

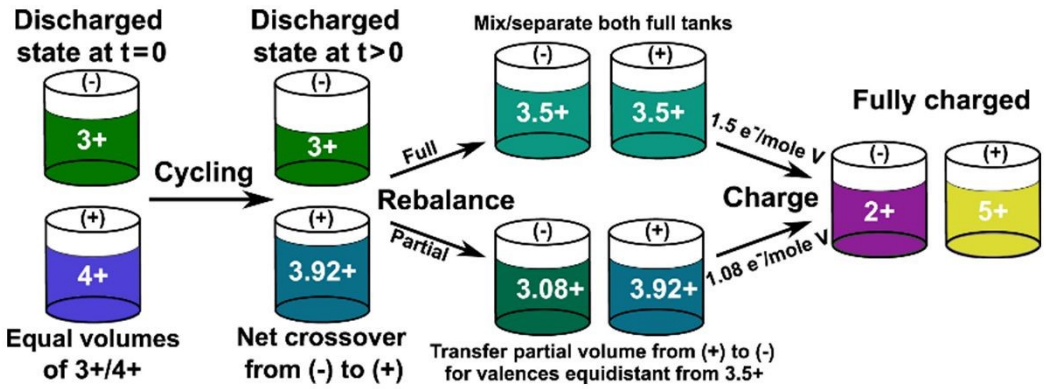

Fig. 21. Schematic of the full and partial rebalancing techniques[26] (Reprinted with permission of Elsevier)

4.2.2 Chemical reduction recovery

The chemical reduction method of electrolyte price recovery includes the method of restoring battery capacity in situ by adding different reducing agents[108]as shown in Fig. 22(a), such as adding ammonium ferrous sulfate[109], ascorbic acid, oxalic acid, formic acid and ethylene glycol to reduce anode V^{5+} electrolyte[110, 111]. The equation of adding oxalic acid as reducing agent is shown in Eq. (23):

$$(VO_2)_2SO_4 + H_2C_2O_4 + H_2SO_4 = 2VOSO_4 + 2H_2O + 2CO_2 \quad (23)$$

View Article Online
DOI: 10.1039/D5SU00532A

After the restoration with oxalic acid[112], as can be seen from the discharge specific capacity curve in Fig. 22(b-c), the capacity decay of the battery significantly slows down after the electrode exchange and restoration. After 130 cycles, the capacity retention rate is 81.8%, which is significantly higher than the retention rate of 64.2% after 100 cycles of the original factory electrolyte. Meanwhile, the Coulombic efficiency and energy efficiency of the battery significantly increase after the electrode exchange and restoration, indicating a remarkable improvement in the electrochemical performance of the electrodes.

The addition of chemical reducing agent to restore the valence state of the positive electrolyte mainly has the problems of imprecise control of the additive amount resulting in residuals, the introduction of impurities, and the need to avoid excessive reduction.

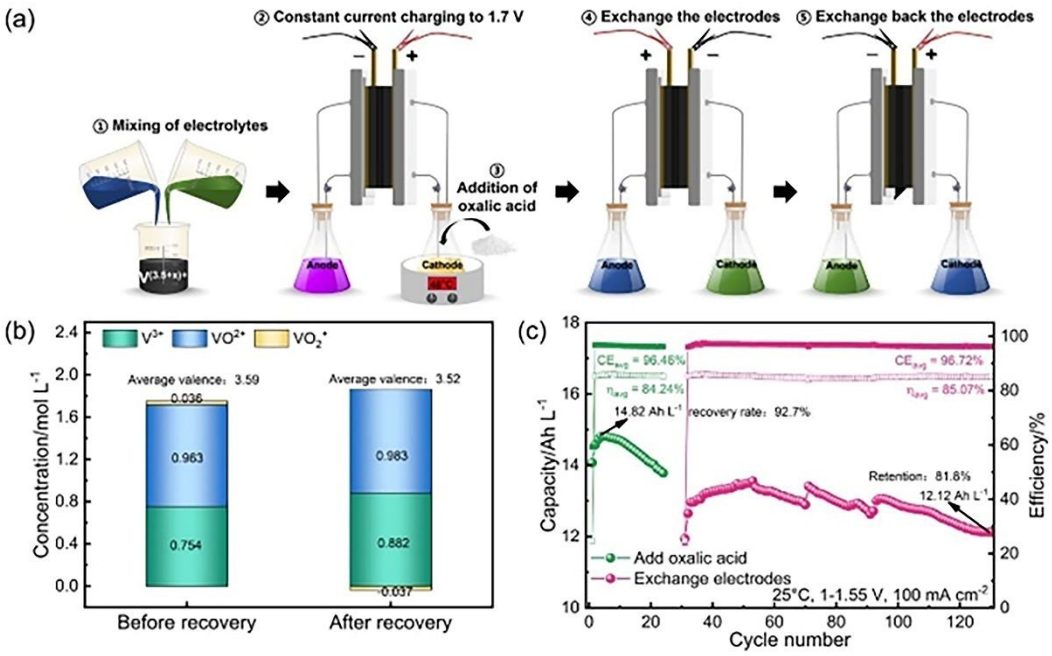

Fig. 22 (a) Schematic diagram; (b) Comparison of electrolyte composition; (c)Discharge specific capacity[112]

View Article Online
DOI: 10.1039/D5SU00532A

4.2.3 Electrolytic recovery

The electrolytic method employs an electrolytic cell structurally similarly to the battery configuration. Oxygen evolution reaction of water molecules at the anode produces O_2, and the cathode reduces V^{5+} in the high-valence vanadium electrolyte with unbalanced valence state after long-term operation to low price, thus restoring the average valence state of the electrolyte[113, 114]. The VFB capacity recovery system is mainly composed of a VFB module and an electrolysis module connected by a pipeline and a flow controller in Fig. 23(a). The positive electrolyte flows from the positive accumulator of VFB through the positive cell, and then returns to the positive accumulator, and the same is true for the negative electrode in Fig. 23(b). The electrolyte flows through the negative storage tank, negative cell, positive storage tank and positive cell of VFB, then flows through the negative cell of electrolytic cell, and finally returns to the negative storage tank of VFB. where the positive and negative electrode electrolytes are combined for in-line electrolysis to extend the cycle life of VFB in Fig. 23(c) This method reduces the average valence state of the mixed electrolyte through electrolysis, while incorporating real-time monitoring of valence state changes to ensure the process reaches the optimal 3.5 valence endpoint. The use of electrolytic restoration can effectively restore the valence state without introducing impurities, but there is a problem that the electrolytic cell set is easily damaged due to untimely gas discharge and excessive pressure difference between the anode and cathode in high-power electrolysis.

View Article Online
DOI: 10.1039/D5SU00532A

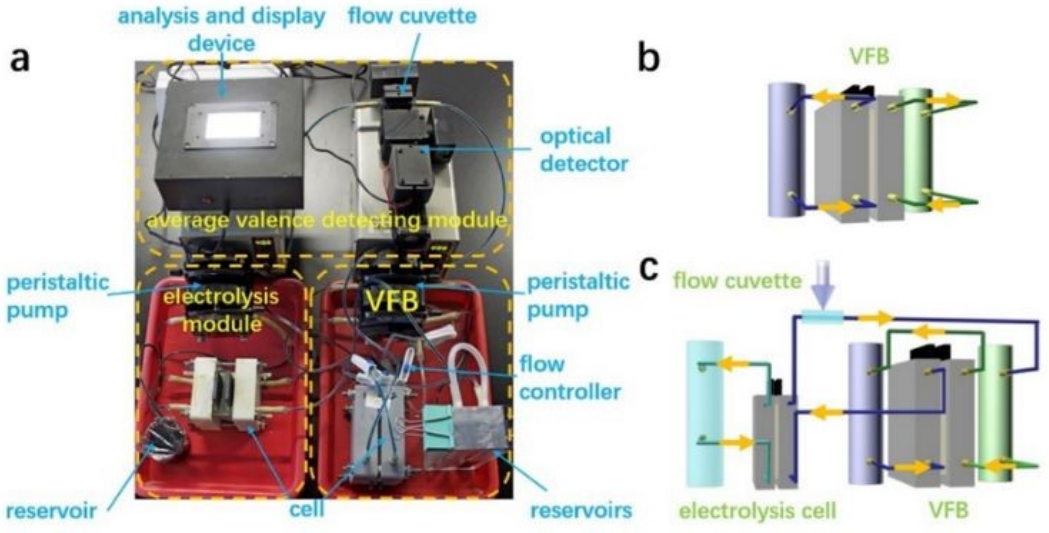

Fig. 23. (a) The photo capacity recovery system.; (b) in the normal mode. (c) in the recovery mode[115] (Reprinted with permission of Elsevier)

5 Conclusions

This review provides a focused analysis on advanced methodologies for preparing $V^{3.5+}$ electrolytes. Comprehensive analysis including chemical reduction method, electrolysis method, chemical reduction-electrolysis method has been conducted. Their chemical principles, processes, advantages and limitations have been evaluated, while the preparation of high-purity $V^{3.5+}$ electrolyte still faces significant challenges. Compared with high-purity $VOSO_4$ and V_2O_5, the selection of vanadium raw materials may have more possibilities. For example, extracting vanadium from vanadium-containing waste to prepare vanadium electrolyte has greater economic benefits and environmental value, and is also of great significance for the sustainable recycling of resources. At present, there is an urgent need for an efficient, stable and low-cost preparation route of $V^{3.5+}$ electrolyte, which can avoid introducing impurities to replace the conventional electrolysis method with high energy consumption and slow kinetics,

View Article Online
DOI: 10.1039/D5SU00532A

the reduction method with possible impurities and the high-cost noble metal catalysts. At the same time, no matter what kind of vanadium raw materials and preparation methods are used, VO_2^+ and VO^{2+} can be converted into $V^{3.5+}$ while ensuring the high purity of products, the cycle life and cost of VFB need to be considered to support its large-scale application in the production of industrial $V^{3.5+}$ electrolyte. The ideal preparation technology of vanadium electrolyte needs three dimensions: environmental friendliness, economic feasibility and the need of social sustainable development.

View Article Online
DOI: 10.1039/D5SU00532A

CRediT authorship contribution statement

Pai Wang: Investigation, Writing – original draft. **Yu Qin**: Conceptualization, Methodology, Writing – review & editing, Project administration. **Fancheng Meng**: Formal analysis, Validation, Writing – review & editing. **Lina Wang:** Supervision, Funding acquisition. **Tao Qi:** Resources.

Declaration of competing interest

The authors declare that they have no known competing financial interests or personal relationships that could have appeared to influence the work reported in this paper.

Data availability

This review article is based solely on previously published data (which can be found in the referenced articles), and no new data were generated.

Acknowledgments

The authors gratefully acknowledge the financial support from Deep Earth Probe and Mineral Resources Exploration-National Science and Technology Major Project (2024ZD1003408) and Strategic Priority Research Program of the Chinese Academy of Sciences (XDA0430103)

View Article Online
DOI: 10.1039/D5SU00532A

References

1. K. C. Divya and J. Østergaard, *Electric power systems research*, 2009, **79**, 511-520.
2. X. Wang, Y. Zhang and H. Zhang, *Journal of Electrochemistry*, 2015, **21**, 433-440.
3. B. Khaki and P. Das, *Electrochimica Acta*, 2022, **405**, 139842.
4. T.-N. Pham-Truong, Q. Wang, J. Ghilane and H. Randriamahazaka, *ChemSusChem*, 2020, **13**, 2142-2159.
5. M. Skyllas-Kazacos, G. Kazacos, G. Poon and H. Verseema, *International Journal of Energy Research*, 2010, **34**, 182-189.
6. Z. Wei, A. Bhattarai, C. Zou, S. Meng, T. M. Lim and M. Skyllas-Kazacos, *Journal of Power Sources*, 2018, **390**, 261-269.
7. M. Kapoor, R. K. Gautam, V. K. Ramani and A. Verma, *Chemical Engineering Journal*, 2020, **379**, 122300.
8. Y.-H. Fu, Y.-Y. Peng, L. Zhao, T.-Q. He, M.-M. Yuan, H. Dang, R. Liu and F. Ran, *Tungsten*, 2024, **6**, 561-573.
9. M. Rychcik and M. Skyllas-Kazacos, *Journal of power sources*, 1988, **22**, 59-67.
10. M. Skyllas-Kazacos, M. Rychcik, R. G. Robins, A. Fane and M. Green, *Journal of the electrochemical society*, 1986, **133**, 1057.
11. J. Zhu, Y. Yuan and W. Wang, *International Journal of Electrical Power Energy Systems*, 2019, **111**, 436-446.
12. M. U. H. Naseer, B. Pan, S. Wang, Y. Lyu, B. Liu, L. Li, J. Qi and H. Du, *Journal of Environmental Chemical Engineering*, 2025, **13**, 118402.
13. M. K. Singh, M. Kapoor and A. Verma, *WIREs Energy and Environment*, 2021, **10**, e393.
14. C. Ding, H. Zhang, X. Li, T. Liu and F. Xing, *The journal of physical chemistry letters*, 2013, **4**, 1281-1294.
15. N. Beriwal and A. Verma, *Environmental Science and Pollution Research*, 2022, **29**, 72187-72195.
16. H. Choi, D. Mandal and H. Kim, *ACS Sustainable Chemistry Engineering*, 2022, **10**, 17143-17150.
17. J. Heo, J.-Y. Han, S. Kim, S. Yuk, C. Choi, R. Kim, J.-H. Lee, A. Klassen, S.-K. Ryi and H.-T. Kim, *Nature communications*, 2019, **10**, 4412.
18. J. Noack, L. Wietschel, N. Roznyatovskaya, K. Pinkwart and J. Tübke, *Energies*, 2016, **9**, 627.
19. C. Minke, U. Kunz and T. Turek, *Journal of Power Sources*, 2017, **361**, 105-114.
20. G. Kear, A. A. Shah and F. C. Walsh, *International journal of energy research*, 2012, **36**, 1105-1120.
21. Y. Guo, J. Huang and J.-K. Feng, *Journal of Industrial Engineering Chemistry*, 2023, **118**, 33-43.
22. X. Zang, L. Yan, Y. Yang, H. Pan, Z. Nie, K. W. Jung, Z. D. Deng and W. Wang, *Small Methods*, 2019, **3**, 1900494.
23. I. Rashitov, A. Voropay, G. Tsepilov, I. Kuzmin, A. Loskutov, A. Kurkin, E. Osetrov and I. Lipuzhin, *Batteries*, 2023, **9**, 464.
24. L. Wu, J. Wang, Y. Shen, L. Liu and J. Xi, *Physical Chemistry Chemical Physics*, 2017, **19**, 14708-14717.

25. R. Pichugov, P. Loktionov, A. Pustovalova, A. Glazkov, A. Grishko, D. Konev, M. Petrov, A. Usenko and A. Antipov, *Journal of Power Sources*, 2023, **569**, 233013.
26. K. E. Rodby, T. J. Carney, Y. A. Gandomi, J. L. Barton, R. M. Darling and F. R. Brushett, *Journal of Power Sources*, 2020, **460**, 227958.
27. B. Khaki and P. J. E. A. Das, 2022, **405**, 139842.
28. L. Li, S. Kim, W. Wang, M. Vijayakumar, Z. Nie, B. Chen, J. Zhang, G. Xia, J. Hu and G. Graff, *Advanced Energy Materials*, 2011, **1**, 394-400.
29. M. Zarei-Jelyani, M. M. Loghavi, M. Babaiee and R. J. J. o. A. E. Eqra, 2024, **54**, 719-730.
30. N. Roznyatovskaya, J. Noack, H. Mild, M. Fühl, P. Fischer, K. Pinkwart, J. Tübke and M. Skyllas-Kazacos, *Batteries*, 2019, **5**, 13.
31. C. Fan, H. Yang and Q. Zhu, *International Journal of Electrochemical Science*, 2017, **12**, 7728-7738.
32. Y. Yang, Y. Zhang, L. Tang, T. Liu, J. Huang, S. Peng and X. Yang, *Journal of Power Sources*, 2019, **434**, 226719.
33. X. Wu, J. Liao, X. Yin, J. Liu, S. Wu, X. Wu, Z. Xie and W. Ling, *Chemical Communications*, 2024, **60**, 2906-2909.
34. R. Aakesson, L. G. Pettersson, M. Sandstroem and U. J. J. o. t. A. C. S. Wahlgren, *Journal of the American Chemical Society*, 1994, **116**, 8691-8704.
35. M. Benmelouka, S. Messaoudi, E. Furet, R. Gautier, E. Le Fur and J.-Y. Pivan, *The Journal of Physical Chemistry A*, 2003, **107**, 4122-4129.
36. M. Vijayakumar, L. Li, Z. Nie, Z. Yang and J. Hu, *Physical Chemistry Chemical Physics*, 2012, **14**, 10233-10242.
37. S. C. Larsen, *The Journal of Physical Chemistry A*, 2001, **105**, 8333-8338.
38. C. V. Grant, W. Cope, J. A. Ball, G. G. Maresch, B. J. Gaffney, W. Fink and R. D. Britt, *The Journal of Physical Chemistry B*, 1999, **103**, 10627-10631.
39. M. Vijayakumar, S. D. Burton, C. Huang, L. Li, Z. Yang, G. L. Graff, J. Liu, J. Hu and M. Skyllas-Kazacos, *Journal of Power Sources*, 2010, **195**, 7709-7717.
40. F. Sepehr and S. J. Paddison, *Chemical Physics Letters*, 2013, **585**, 53-58.
41. M. Bühl and M. Parrinello, *Chemistry–A European Journal*, 2001, **7**, 4487-4494.
42. J. Krakowiak, D. Lundberg and I. Persson, *Inorganic chemistry*, 2012, **51**, 9598-9609.
43. H.-J. Hong, H. S. Kim and Y. J. Suh, *Industrial Engineering Chemistry Research*, 2022, **61**, 11139-11147.
44. S. Gupta, N. Wai, T. M. Lim and S. H. Mushrif, *Journal of Molecular Liquids*, 2016, **215**, 596-602.
45. H. Peng, D. Tang, M. Liao, Y. Wu, X. Fan, B. Li, H. Huang and W. Shi, *Metals*, 2022, **12**, 557.
46. P. Hu, Y. Zhang, J. Huang, T. Liu, Y. Yuan and N. Xue, *ACS Sustainable Chemistry Engineering*, 2018, **6**, 1900-1908.
47. X. Chen, J. Zhang and B. Yan, *Minerals Engineering*, 2021, **165**, 106864.
48. G. Park, Y. Lim, K. Hyun and Y. Kwon, *Journal of Power Sources*, 2024, **589**, 233770.
49. S. Das, S. Chakraborty, O. Parkash, D. Kumar, S. Bandyopadhyay, S. Samudrala, A. Sen

View Article Online
DOI: 10.1039/D5SU00532A

and H. S. Maiti, *Talanta*, 2008, **75**, 385-389.
50. A. R. Petersen, L. B. Nielsen, J. R. Dethlefsen and P. Fristrup, *ChemCatChem*, 2018, **10**, 769-778.
51. K. Wang, Y. Zhang, L. Liu, J. Xi, Z. Wu and X. Qiu, *Electrochimica Acta*, 2018, **259**, 11-19.
52. S. Sun, L. Fang, H. Guo, L. Sun, Y. Liu and Y. J. S. Cheng, *Advanced Science*, 2023, **10**, 2207728.
53. W. Wang, X. Fan, J. Liu, C. Yan and C. Zeng, *Journal of Power Sources*, 2014, **261**, 212-220.
54. J. Xi, S. Xiao, L. Yu, L. Wu, L. Liu and X. Qiu, *Electrochimica Acta*, 2016, **191**, 695-704.
55. S. Xiao, L. Yu, L. Wu, L. Liu, X. Qiu and J. Xi, *Electrochimica Acta*, 2016, **187**, 525-534.
56. Y. Zeng, T. Zhao, L. An, X. Zhou and L. Wei, *Journal of Power Sources*, 2015, **300**, 438-443.
57. Z. Wang, Z. Qin, L. Chen, B. Liang, Y. Zhu, K. Wu and D. Luo, *Process Safety Environmental Protection*, 2023, **174**, 298-309.
58. D. He, Q. Feng, G. Zhang, L. Ou and Y. Lu, *Minerals Engineering*, 2007, **20**, 1184-1186.
59. R. Liu, J. Pan, X. Xie, S. Wang, J. Wang and T. Zhou, *Journal of Chemical Engineering of Chinese Universities*, 2014, **28**, 1275-1280.
60. X. Hui, Y. Xingrong and W. Xuewen, *CN201711295760.X (Chinese Patent)*, 2022, 16.
61. N. Andriopoulos, L. CE, R. Dukino and M. SJ, *ISIJ international* 2003, **43**, 1528-1537.
62. W. M. Carvalho, L. Cassayre, D. Quaranta, F. Chauvet, R. El-Hage, T. Tzedakis and B. Biscans, *Journal of Energy Chemistry*, 2021, **61**, 436-445.
63. J. Martin, K. Schafner and T. J. E. T. Turek, 2020, **8**, 2000522.
64. W. Li, R. Zaffou, C. C. Sholvin, M. L. Perry and Y. She, *ECS Transactions*, 2013, **53**, 93.
65. Y. Hu, Y. Zhang, N. Xue and P. Hu, *Separation and Purification Technology*, 2024, **338**, 126496.
66. Z. Li, C. Wu and H. Wan, *Springer International Publishing*, 2022, 470-478 , DOI:410.3969/j.issn.1003-9015.2014.3906.3015(in Chinese).
67. C. Wang, L.-J. Li and H. Du, *Tungsten*, 2024, **6**, 555-560.
68. C. Hu, Y. Dong, W. Zhang, H. Zhang, P. Zhou and H. Xu, *Journal of Power Sources*, 2023, **555**, 232330.
69. C. Hu, Y. Dong, W. Zhang, H. Zhang, P. Zhou and H. Xu, *Journal of Power Sources*, 2023, **555**.
70. N. H. Choi, S.-k. Kwon and H. Kim, *Journal of the Electrochemical Society*, 2013, **160**, A973.
71. A. A. Pustovalova, P. A. Loktionov, I. O. Speshilov, R. D. Pichugov, A. Y. Grishko, A. T. Glazkov and A. E. Antipov, *Journal of Power Sources*, 2023, **576**, 233211.
72. T. Sukkar and M. Skyllas-Kazacos, 2003, **222**, 235-247.
73. J. Martin, K. Schafner and T. Turek, *Energy Technology*, 2020, **8**, 2000522.
74. S. Niu, H. Li, H. Guo, Y. Liu and Y. J. S. Cheng, 2024, **20**, 2405827.
75. E. B. Agyekum, M. Abdullah, F. Odoi-Yorke, A. Ameen, P. Chowdhury, M. A. Raza, F.

View Article Online
DOI: 10.1039/D5SU00532A

1 L. Rashid and A. K. Hussein, *Energy Conversion and Management: X*, 2025, **27**, 101180.
2 76. Y. Wen, Y. Xu and J. Cheng, *CN201310542929.2(Chinese Patent)*, 2015, 6.
3 77. W. M. Carvalho Jr, L. Cassayre, D. Quaranta, F. Chauvet, R. El-Hage, T. Tzedakis and
4 B. J. J. o. E. C. Biscans, 2021, **61**, 436-445.
5 78. Q. Aimiao, Q. Guo, C. Wang, A. Qin, X. J. Q. Chen, C. Wang, A. Qin and X. Chen,
6 *SSRN Electronic Journal*, 2022.
7 79. W. Tian, H. Du, J. Wang, J. J. Weigand, J. Qi, S. Wang and L. Li, *Materials*, 2023, **16**,
8 4582.
9 80. Y. Yadong, Z. Yimin, H. Jing, L. Tao and Z. Qiushi, *Chemical Industry Engineering*
10 *Progress*, 2017, **36**, 274.
11 81. B. Liu, Y. Guo and X. Bi, *CN202310512028.2(Chinese Patent)*, 2023, 8.
12 82. W. Gao, Z. Sun, H. Cao, H. Ding, Y. Zeng, P. Ning, G. Xu and Y. Zhang, *Journal of*
13 *Cleaner Production*, 2020, **256**, 120217.
14 83. D. Li, D. Chen and G. Zhang, *Metals*, 2017, **7**, 106 , Doi:110.3390/met7030106 (in
15 Chinese).
16 84. X. Zhang, F. Meng, Z. Zhu, D. Chen, H. Zhao, Y. Liu, Y. Zhen, T. Qi, S. Zheng and M.
17 Wang, *Hydrometallurgy*, 2022, **208**, 105805.
18 85. H. Liu, Y.-M. Zhang, J. Huang and T. Liu, *Frontiers of Chemical Science and*
19 *Engineering*, 2023, **17**, 56-67.
20 86. Y. Wang, Y. Liu, F. Meng, J. Zhang, S. Zhao, X. Tian, L. Wang, D. Chen and T. Qi,
21 *Separation and Purification Technology*, 2025, **354**, 129281.
22 87. C. Li, T. Jiang, J. Wen, G. Yang, T. Yu, L. Zhang, X. An, G. Hao and X. Liu, *Chemical*
23 *Engineering Journal*, 2025, **511**, 162151.
24 88. M. U. H. Naseer, S. Wang, B. Liu, Y. Lyu, C. Bingxu, C. Wang, B. Pan and H. Du,
25 *Separation and Purification Technology*, 2024, **340**, 126777.
26 89. Y.-W. Hu, Y.-M. Zhang, T. Liu and H. Liu, *Journal of Cleaner Production*, 2023, **394**,
27 136389.
28 90. H. Liu, Y.-m. Zhang, T. Liu, J. Huang, L.-m. Chen and Y.-w. Hu, *Transactions of*
29 *Nonferrous Metals Society of China*, 2023, **33**, 1594-1608.
30 91. C. Liu, T. Liu, Y. Zhang, Z. Dai and Y. Yang, *Separation and Purification Technology*,
31 2020, **240**, 116582.
32 92. Y. Zhang, D. Dreisinger, T.-A. Zhang, G. Lv, W. Zhang and F. Xie, *Hydrometallurgy*,
33 2019, **188**, 54-63.
34 93. Z. Wang, L. Chen, R. Yin, Z. Li, G. Deng, B. Liang, Y. Zhu, K. Wu and D. Luo,
35 *Hydrometallurgy*, 2023, **222**, 106146.
36 94. M. U. H. Naseer, S. Wang, B. Liu, Y. Lyu, C. Bingxu, C. Wang, B. Pan, H. J. S. Du and
37 P. Technology, 2024, **340**, 126777.
38 95. N. Blume, O. Zielinski, M. Becker and C. Minke, *Energy Technology*, 2024, **12**, 2300750.
39 96. M. Kapoor, N. Beriwal and A. Verma, *Journal of Energy Storage*, 2020, **32**, 101759.
40 97. M. Skyllas-Kazacos and L. Goh, *Journal of membrane science*, 2012, **399**, 43-48.
41 98. Y. Wang, A. Mu, W. Wang, B. Yang and J. Wang, *ChemSusChem*, 2024, **17**, e202301787.
42 99. Z. Wang, Z. Guo, J. Ren, Y. Li, B. Liu, X. Fan and T. Zhao, *ACS Central Science*, 2023,
43 **9**, 56-63.
44 100. K. Oh, S. Won and H. Ju, *Electrochimica Acta*, 2015, **181**, 238-247.

View Article Online
DOI: 10.1039/D5SU00532A

101. C. Sun, J. Chen, H. Zhang, X. Han and Q. J. J. o. P. S. Luo, 2010, **195**, 890-897.
102. Q. Luo, L. Li, W. Wang, Z. Nie, X. Wei, B. Li, B. Chen, Z. Yang and V. Sprenkle, *ChemSusChem*, 2013, **6**, 268-274.
103. C. Choi, S. Kim, R. Kim, Y. Choi, S. Kim, H.-y. Jung, J. H. Yang and H.-T. Kim, *Renewable Sustainable Energy Reviews*, 2017, **69**, 263-274.
104. X.-G. Yang, Q. Ye, P. Cheng and T. S. Zhao, *Applied energy*, 2015, **145**, 306-319.
105. Y. Zhang, L. Liu, J. Xi, Z. Wu and X. Qiu, *Applied Energy*, 2017, **204**, 373-381.
106. R. M. Darling, A. Z. Weber, M. C. Tucker and M. L. Perry, *Journal of The Electrochemical Society*, 2015, **163**, A5014.
107. K. Wang, L. Liu, J. Xi, Z. Wu and X. Qiu, *Journal of Power Sources*, 2017, **338**, 17-25.
108. L. Wei, X. Fan, H. Jiang, K. Liu, M. Wu and T. Zhao, *Journal of Power Sources*, 2020, **478**, 228725.
109. D. Shi, H. Zhang and X. Li, *CN201510927447.8 (Chinese Patent)*, 2020, 6.
110. P. Loktionov, R. Pichugov, D. Konev and A. Antipov, *Electrochimica Acta*, 2022, **436**, 141451.
111. Z. Zhao, H. C. Liu and Q. Ge, *CN202310659813.0(Chinese Patent)* , 2023, 11.
112. Y. Tao, W. Yijun and T. Zilong, *Energy Storage Science and Technology*, 2025, **14**, 1177-1186, DOI: 1110.19799/j.cnki.12095-14239.12024.10838 (in Chinese).
113. J. Chen, H. Zhang and C. Sun, *CN200810012119.5(Chinese Patent)*, 2010, 24.
114. Z. Li, J. Xi, L. Liu, Z. Wu and D. Li, *ACS Sustainable Chemistry & Engineering*, 2020, **8**, 10275-10283.
115. R. Gundlapalli and S. Jayanti, *J. Energy Storage*, 2019, **23**, 148.

View Article Online
DOI: 10.1039/D5SU00532A

This review article is based solely on previously published data (which can be found in the referenced articles), and no new data were generated.